

An advanced tool integrating failure and sensitivity analysis to novel modeling for stormwater flooding volume

Francesco Fatone¹, Bartosz Szeląg², Przemysław Kowal³, Arthur McGarity⁴, Adam Kiczko², Grzegorz Wałek⁵, Ewa Wojciechowska³, Michał Stachura⁶, Nicolas Caradot⁷

¹ Department of Science and Engineering of Materials, Environment and Urban Planning-SIMAU, Polytechnic University of Marche Ancona, 60121 Ancona, Italy

² Institute of Environmental Engineering, Warsaw University of Life Sciences-SGGW, 02-797 Warsaw, Poland

³ Faculty of Civil and Environmental Engineering, Gdansk University of Technology, 80-233, Gdansk, Poland

⁴ Department of Engineering, Swarthmore College, 500 College Ave., Swarthmore, PA, 19081, United States

⁵ Institute of Geography and Environmental Sciences, Jan Kochanowski University in Kielce, 25 – 406, Kielce, Poland

⁶ Faculty of Law and Social Sciences, Jan Kochanowski University, 25 – 406, Kielce, Poland

⁷ Berlin Competence for Water, Cicerostr. 24, 10709 Berlin, Germany

Correspondence to: Bartosz Szeląg (bszelag@tu.kielce.pl)

Abstract. An innovative tool for modelling specific flood volume was presented, which can be applied to assess the need for stormwater network modernisation as well as for advanced flood risk assessment. Field measurements for a catchment area in Kielce, Poland were used to apply the model and demonstrate its usefulness. This model extends the capabilities of recently developed statistical and/or machine learning hydrodynamic models developed from multiple runs of the U.S. EPA's Storm Water Management Model (SWMM) model. The extensions enable inclusion of: 1) characteristics of the catchment, and its stormwater network, calibrated model parameters expressing catchment retention and the capacity of the sewer system, (2) extended sensitivity analysis and (3) risk analysis. Sensitivity coefficients of calibrated model parameters include correction coefficients for percentage area, flow path, depth of storage, impervious area, Manning roughness coefficients for impervious areas, and Manning roughness coefficients for sewer channels. Sensitivity coefficients were determined with regard to rainfall intensity and characteristics of the catchment and stormwater network. Extended sensitivity analysis enabled an evaluation of the variability of the specific flood volume and sensitivity coefficients within a catchment, in order to identify the most vulnerable areas threatened by flooding. Thus, the model can be used to identify areas particularly susceptible to stormwater network failure and the sections of the network where corrective actions should be taken to reduce the probability of system failure. The developed simulator to determine a specific flood volume represents an alternative approach to the SWMM model that, unlike current approaches, is calibratable with limited topological data availability, therefore generates a lower cost due to the less amount and specificity of data required.

36 **Highlight**

- 37 • simulator of a specific volume of flood as an alternative to the SWMM model,
- 38 • sensitivity analysis extension considering rainfall and catchment topological data,
- 39 • the probability of failure of the stormwater system as a criterion for corrective actions under conditions of uncertainty

41 **1. Introduction**

42 Climate change and urbanization are the main factors increasing the pressure on the functioning of sewer networks,
43 in particular components responsible for stormwater management (Miller et al., 2014; Hettiarachchi, et al, 2018; Lama et al.
44 2021a; Khan et al, 2022). This results in an increase in the frequency and volume of stormwater flooding, deterioration of the
45 living standards of the inhabitants, and pipes abrasion (Jiang et al., 2018; Zhou et al. 2018; Chang et al. 2020; Lense et al.
46 2023). The literature data (Siekmann et al. 2011) shows that the basis for making decisions on corrective actions (replacement
47 of a pipe, removal of sediments, construction of a reservoir, etc.) is the specific flood volume expressing the volume of
48 stormwater flooding on a unit impervious surface. Limiting values for the specific flood volume have been determined by
49 Siekmann and Pinnekamp (2011), based on simulations for urban catchments, as the basis for the maintenance of the sewage
50 network and the criterion for making decisions on modernization or corrective actions.

51 In order to obtain a required hydraulic efficiencies, simulation models are typically used to plan corrective actions
52 (Kirshen et al. 2014). For this purpose, mechanistic models are used, such as the USEPA's Storm Water Management Model
53 (SWMM), which account for surface runoff, drainage of the sewage network, and flooding of stormwater during system
54 overload (Guo et al. 2021; Li et al. 2022; Yang et al., 2022; Lama et al. 2021b). As in the case with other mechanistic models
55 (MOUSE, PCSWMM, MIKE URBAN etc.), SWMM can incorporate the spatial characteristics of a sewage network, as well
56 hydraulic conditions, in calculations that predict and characterize stormwater flooding (Martins et al. 2018; Yang et al., 2020;
57 Ma et al., 2022). However, such models are characterized by high specificity (one model can be used for one catchment), and
58 they require the collection of detailed data and measurements (rainfall, runoff), which is labour-intensive and generates high
59 costs. Moreover, there are a strong interactions between the calibrated parameters (Wu et al. 2013; Chen et al. 2018; Sonavane
60 et al. 2020; Shrestha et al., 2022; Ray et al. 2023), leading to uncertainty of simulation results (Ball 2020; Kobarfard et al.
61 2022; Sun et al. 2022) which complicates to select specified corrective action (Kim et al. 2017; Bobovic et al. 2018; Hung and
62 Hobbs 2018). To solve this problem, an important step in the development of the computational algorithm is the
63 implementation of sensitivity analysis (Fraga et. al. 2016; Cristiano et al. 2019; Razavi and Gupta 2019). Simulations by Szeląg
64 et al. (2021) have shown the influence of uncertainty in calibrated SWMM parameters on the calculation of specific flood
65 volume and degree of flooding, which was also confirmed by the simulations of Fraga et al. (2016) and Kelleher et al. (2017).

66 To overcome the limitations of MCM, the implementation of statistical and/or machine learning methods seems is a
67 prospective alternative (Rosenzweig et al. 2021; Lei et al. 2021; Bui et al. 2019; Shafizadeh-Moghadam et al. 2018; Chen et
68 al. 2019; Fong and Chui, 2020; Mohammand et al. 2023). ML methods can estimate-of specific stormwater flood volume for
69 a catchment area with different topology. However, so far, no simulator model based on statistical and/or machine learning

70 has been developed to simulate specific stormwater flood volume while taking into account the factors included in mechanistic
71 models (Mignot et al., 2019; Guo et al. 2021; Rosenzweig et al. 2021). Some progress in application of machine learning
72 methods to simulation of stormwater flooding has been made. Thorndahl et al. (2008), based on simulation results of flooding
73 from manholes, including uncertainty of calibrated parameters, developed a model using the FORM (first order reliability
74 model) method. Jato-Espino et al. (2018) and Li and Willems (2020), conducting simulations with mechanistic models, present
75 models (logistic regression) for identification of flooding from a single manhole based on rainfall frequency, catchment and
76 stormwater network characteristics. Therefore, Szeląg et al. (2022a, 2022b) proposed a models for calculating estimates of
77 stormwater flooding in a catchment, but due to insufficient data in constructing the model, application is limited. In the
78 aforementioned models, interactions between land use, catchment and stormwater network characteristics, as well as system
79 capacity were neglected. However, by omitting these factors, at the spatial planning stage, reduces the applicability of the
80 model.

81 Another important indicator of proper sewage network management is the assessment of the risk of system failure
82 (exceed the maximum specific flood volume). Reliable risk assessment requires the integration of mechanistic models,
83 statistical approach and simulators of rainfall data (Fu et al. 2012; Zhou et al. 2019; Venvik et al. 2020). Most of the methods
84 (Ursino 2014; Cea and Costabile 2022; Taromideh et al. 2022) focus on determining the impact of climatic changes in rainfall
85 on the efficiency of the sewage system and include the impact of parameters expressing terrain and sewer retention. Currently,
86 there is no effective method of risk analysis taking into account the uncertainty of the calibrated parameters to simulate a
87 specific flood volume for the different urban catchments.

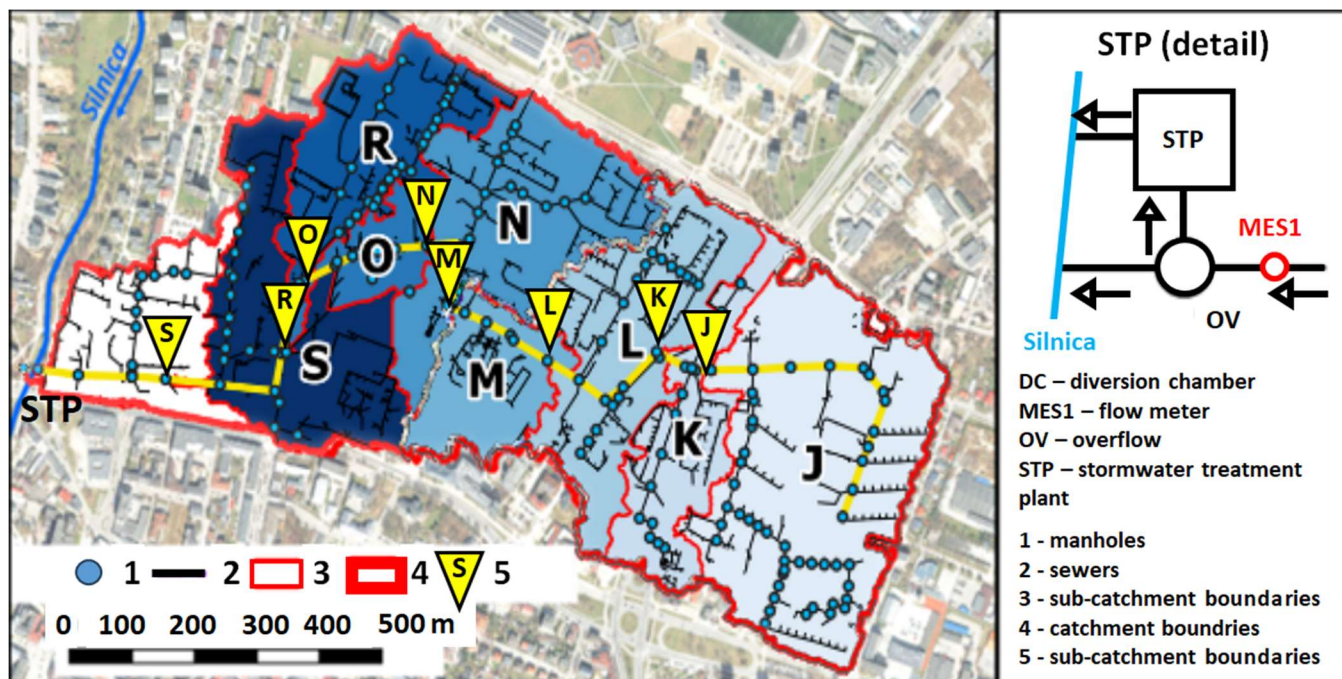
88 The aim of the article was to develop an innovated simulator, combined with risk assessment and sensitivity analyses
89 for calculating the specific flood volume, taking into account rainfall data, catchment characteristics and topology. Recognition
90 of the above factors enabled the application of the proposed logistic regression model to identify stormwater flooding in
91 catchments with different characteristics, as an alternative approach to the SWMM model. An important aspect of the proposed
92 approach was the risk assessment of system failure (specific volume of flood exceed $13 \text{ m}^3 \cdot \text{ha}^{-1}$) and sewage system operation
93 under uncertainty. Moreover, the methodology presented in the work, integrated with the stormwater flooding simulator,
94 enabled the identification of the impact of calibrated SWMM parameters on the results of the sensitivity analysis in catchments
95 with different characteristics. This feature enables building a mechanistic model, which allows appropriate selection of
96 techniques for measuring input data, which can ultimately reduce the costs of applying the model. The developed methodology
97 enables the appropriate selection of devices for measuring the flow rate, and their location in the sewage network in the context
98 of calibrating the catchment model and reducing the costs of flow measurements.

99

100 **2. Case study**

101 The analysed urban catchment is located in the south-eastern part of Kielce, central Poland, Świętokrzyskie region
102 (Figure 1). Residential districts, public buildings, main and side streets are located in the study area. The catchment area covers
103 63 ha and consists of 40% impervious and 60% permeable areas. The road density is $108 \text{ m} \cdot \text{ha}^{-1}$ (Wałek, 2019), and the terrain

104 denivelation is 11.20m (the ordinates of the highest and the lowest points of the terrain are 271.20 m and 260 m above sea
105 level, respectively).



106
107
108

Figure. 1. Study catchment area (Walek, 2019).

109 The length of the main interceptor channel in the stormwater network is 1569 m, with an average slope of 0.71%. The diameter
110 of the main interceptor expands from 600 to 1250 mm, while the diameters of side sewers vary between 300 and 1000 mm.
111 The slope of the sewers varies between 0.04 and 3.90%. The analysed stormwater system is separated from the municipal
112 sewage. Stormwater flows to the division chamber (DC), and after reaching a depth of 0.42 m it flows into a stormwater
113 treatment plant (STP). During heavy rainfall, when the stormwater level in the DC exceeds the overflow level (OV), it is
114 discharged by the storm overflow (OV) into the S1 channel, which transports the stormwater directly to the Silnica river
115 (without treatment). At a 3.0 m distance from the inlet of the main interceptor to the DC, the flow meter MES1 is installed,
116 which measures the flow rates during heavy rainfall with resolution of 1 minute. Analysis of data from 2010–2020 showed
117 that during dry periods the measured flow rates varied between 1–9 $\text{dm}^3 \cdot \text{s}^{-1}$, which indicates that infiltration occurs in the
118 stormwater network. Measurements of stormwater network operation carried out in the years 2008–2019 indicated that
119 stormwater flooding occurs in the analysed catchment. Taking into account, 159 episodes of rainfall – runoff, within four
120 catchments, 23 cases of flooding were observed. At a distance of 2.5 km from the catchment boundary, a rainfall measurement
121 station is located, which provides constant measurement of rainfall, with a 1-minute temporal resolution.

122

123 *Sub-catchment division and characteristics*

124 The analysed catchment was divided into sub-catchments (Szeląg et al. 2022), which constituted study areas for
 125 identification of stormwater flooding. Due to limited amount range of rainfall data, the obtained model for simulation of
 126 stormwater overflow did not include all important factors, such as dry period duration between rainfall events, retention
 127 catchment that impact flooding phenomenon, which meant that the model had limited predictive capability. Detailed
 128 description and justification of sub-catchments used for construction of flooding identification model was presented by Szeląg
 129 et al. (2022). In reference to approach proposed by Duncan et al. (2011), Jato – Espino et al. (2018), Li and Willems (2022),
 130 in the current analysis the number of sub-catchments used for development of a logit model was increased to 8 (Figure 2). The
 131 sub-catchments boundaries together with data on spatial development and stormwater network (Table 1) were determined
 132 based on maps for design purposes, which was discussed in detail by Szeląg (2013).

133
 134 **Table 1. Characteristics of sub-catchments**

No.	F	Imp	Vk	Gk	R.t.	Vkp	dH1	dHp	Lk	Jkp	Hst	Impd	Gkd	Vrd	Vkd
	ha	-	m ³	m·ha ⁻¹	m	m ³	m	m	m	-	m	-	m·ha ⁻¹	m ³	m ³
J	12.66	0.37	157.0	0.0079	1.74	33.2	0.24	0.25	96.5	0.0036	1.42	0.40	0.0072	2159.4	2577.2
K	18.92	0.38	360.4	0.0084	1.69	28.4	0.31	1.05	56.5	0.0055	2.36	0.40	0.0063	1886.8	2373.7
L	27.15	0.36	557.4	0.0074	2.74	29.6	0.34	1.75	59.0	0.0058	2.36	0.42	0.0053	1496.0	2176.7
M	29.78	0.36	678.8	0.0068	4.49	48.7	0.38	1.15	62.0	0.0061	2.32	0.43	0.0050	1373.3	2055.3
N	36.78	0.37	712.2	0.0081	4.49	48.7	0.38	1.15	62.0	0.0061	2.32	0.44	0.0040	1061.4	2022.0
O	41.31	0.32	858.2	0.0079	5.32	16.1	0.21	1.28	20.5	0.0102	2.31	0.49	0.0037	825.9	1876.0
P	45.42	0.37	981.9	0.0082	5.64	16.1	0.21	1.28	20.5	0.0102	2.31	0.46	0.0027	682.2	1752.3
R	48.31	0.37	981.9	0.0088	5.64	16.1	0.21	1.28	20.5	0.0102	2.31	0.47	0.0023	553.1	1752.3
S	55.41	0.41	1240.2	0.0092	8.47	67.5	0.67	1.8	86.0	0.0078	2.31	0.55	0.0011	258.4	1493.9

135 where: F – catchment surface area; Imp – impervious area; Vk – volume of stormwater channel; Gk – length of stormwater
 136 channel per impervious area of the catchment; R.t. – height difference of the channel, Vkp – volume of the channel above the
 137 cross-section of a catchment; dH1 – height difference of the terrain at section above cross-section r; dHp – height difference
 138 at section above cross-section; Lk – length of channel above cross-section of a catchment; Jkp – channel slope above cross-
 139 section of a catchment; Hst – the height of a manhole at cross-section; Imp – impervious area of downstream area; Gkd –
 140 length of a channel per impervious area below cross-section; Vrd – catchment retention above the cross-section calculated as
 141 $Vrd = F \cdot (Imp \cdot d_{imp} + (1 - Imp) \cdot d_{per})$, Vkd – total retention of a catchment.

142
 143 Data were verified using independent analysis performed by Wałek (2019), who used Qgis program to develop spatial
 144 development model and stormwater network for Kielce. Location of closing cross-sections of sub-catchments (J, K, L, M, M,
 145 O, P, R, S) along the main interceptor were additionally supported by simulation results of outflow hydrographs developed by
 146 Wałek (2019) with use of HEC-HSM model as well as by Szeląg et al. (2014, 2022) with use of hydrodynamic model SWMM.

147 3. Methodology

148

149 3.1. Criterion for stormwater system operation and modernisation

150 The value of a specific flood volume was defined as stormwater flooding per paved area, which can be expressed by
151 the following formula (Sinekamp and Pinekamp, 2011):

$$152 \quad \kappa = \frac{\sum_{i=1}^K V_{t(i)}}{A_{pav}} \quad (1)$$

153 where: V_i – volume of stormwater flooding from i -th manhole of the stormwater network, K – number of manholes, A_{pav} –
154 paved area. Sinekamp and Pinekamp (2011) based on continuous simulations with hydrodynamic models for 3 urban
155 catchments found that the specific flood volume ranged from 0 - (>20) $\text{m}^3 \cdot \text{ha}^{-1}$.

156

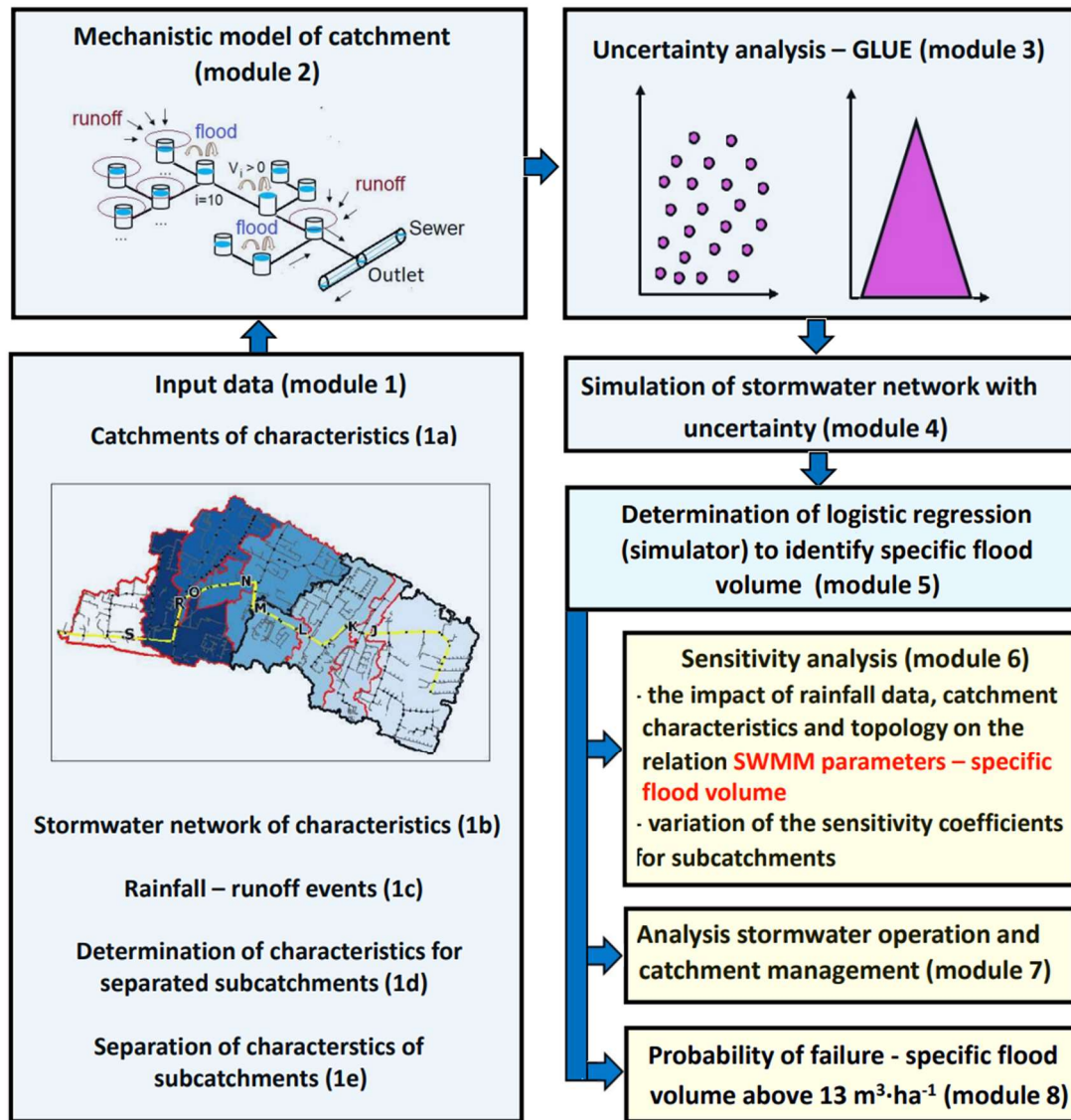
157 On this basis, they established limiting κ values expressing the need to improve the operating conditions of the drainage system.
158 They showed that for $\kappa > 13 \text{ m}^3 \cdot \text{ha}^{-1}$ the drainage system requires adaptation This was also confirmed by the calculations of
159 Kotowski et al. (2014) for the catchment in Wroclaw and Szeląg et al. (2021) for the catchment in Kielce. This allows us to
160 conclude for urban catchments (Poland, Germany) that the κ value quoted above can be a criterion for making decisions on
161 corrective actions of the drainage network.

162

163 3.2. Simulator structure and development

164 The concept of the proposed of tool based on simulator integrated with the risk assessment and sensitivity analysis to
165 evaluate operation of sewage system was presented in Figure 2. Applying the MCM of an urban catchment with separate sub-
166 catchments (varying land use and topology), a simulator of the specific flood volume was developed as an alternative approach
167 to the SWMM. A proposed simulator of logistic regression model-based on rainfall data, catchment and stormwater network
168 characteristics, SWMM parameters (width of runoff path, retention depth of impervious areas, Manning roughness coefficient
169 of impervious areas, correction coefficient of impervious areas, Manning roughness coefficient of channels). The resulting
170 tool enables fast analysis of sewer network performance even with limited data access and can be applied to other catchments.
171 Proposed methodology is based on extension of algorithms given by Szeląg et al. (2021, 2022). In contrast to previous studies
172 (Szeląg et al. 2022), the current approach took into account the retention of the catchment and the sewer network, and the
173 performance criterion of the sewer network was the volume of flooding and not just the fact that it occurred. Integration of the
174 simulator with an analytical relationship for sensitivity coefficient calculations for logistic regression allows fast evaluation of
175 the impact of MCM parameters on flooding for arbitrary catchment characteristics and topological data.

176



177

178 **Figure. 2. Algorithm for developing an advanced tool to simulate a specific flood volume (situation maps in module**
 179 **(1a), (1b) by Walek (2019).**

180
 181 In order to provide more reliable simulation results, the proposed risk assessment took into account the uncertainty of the
 182 SWMM parameters and enabled the optimisation of the operation of the sewer network based on the maximum allowable
 183 values of the channel Manning roughness coefficients.

184

185

186

187 3.3. Algorithm structure

188 The proposed computation algorithm consists of 9 modules. Modules 1, 2, 3, 4 include identical steps as in the work
189 of Szeląg et al. (2021, 2022). In the present study, the scope of the analyses was extended, as in addition to precipitation data
190 and SWMM parameters (Szeląg et al. 2022), the characteristics of the catchment and the stormwater network of the separated
191 sub-catchments were also included (module 1), which was used to determine the computational model. On the basis of spatial
192 data (1a, 1b), a mechanistic model of the catchment was built (module 2), which allowed to perform an uncertainty analysis
193 using the GLUE method (module 3). On this basis, simulations were performed in separated sub-catchments for rainfall events
194 (1e) under uncertainty (module 4). Based on the simulation results a logistic regression model was developed (module 5) to
195 calculate the local sensitivity coefficients for calibrated SWMM parameters, with regard to rainfall intensity and catchment
196 characteristics (module 6). Modules 1, 2, 3, 4 included analyses to determine a specific flood volume simulator that can be
197 applied to any catchment. Thus, future algorithm implementation for the new catchment, will ultimately include only modules
198 6, 7, 8. Using adopted rainfall data, the sensitivity coefficients of SWMM model parameters for sub-catchments are computed
199 and maps showing sensitivity changes in catchment scale are drawn (module 6). While the model is applied to identify
200 stormwater flooding, the possible methods for improving stormwater network operating are analysed inside module 7, 8.
201 Computations using the developed algorithm consist of the following steps:

202 1) collecting of the input data (catchment characteristics – 1a, stormwater network characteristics – 1b, rainfall – runoff
203 episodes – 1c), separation of independent rainfall episodes – 1d, division and determination of characteristic of sub-catchments
204 – 1e,

205 2) development of hydrodynamic model (module 2) based on catchment characteristics (1a) and stormwater network
206 characteristics (1b),

207 3) conducting of uncertainty analysis with GLUE method (section 3.3.3) using hydrodynamic model of a catchment based on
208 rainfall – runoff episodes (1d),

209 4) using independent rainfall events (1d) simulations with hydrodynamic model including uncertainty of calibrated parameters
210 according to points (4a, 4b, 4c) are conducted;

211 a) simulation of SWMM parameters (*a posteriori distribution*) in Table S1 using the results of uncertainty analysis,

212 b) simulation of stormwater network operation during independent rainfall events (1d) including uncertainty (4a),

213 c) computation of specific flood volume in each sample of independent rainfall events in sub-catchments;

214 transformation of determined κ values to classification data (section 4a),

215 5) determination of logistic regression simulator SWMM of specific flood volume as alternative to MCM model based on
216 results of computations in point 4c,

217 6) sensitivity analysis:

218 a) computations of sensitivity coefficients (with regard to SWMM parameters) for assumed rainfall data and catchment
219 characteristics,

220 b) computations of sensitivity coefficients for sub-catchments (J, K, L, M, N, O, P, R, S),

- 221 7) application of developed logistic regression model for amelioration of stormwater network operation,
222 a) analysis of the impact of corrective variants on sensitivity coefficients in sub-catchments,
223 8) analysis of failures occurrence.

224

225 3.3.1. Determination of independent rainfall events (module 1e)

226 Determination of independent rainfall events for the period 2010 - 2021 was based upon criteria defined in DWA A-
227 118 (2006) guidelines. The minimum time period between independent rainfall events was set as 4.0 hours. Computation of
228 stormwater flooding was performed for rainfall events with a minimum depth of $P_t = 5.0$ mm (Fu and Butler, 2014) and only
229 for those events that resulted from convection rainfalls (i.e., rainfall duration below 120 min). For the analysed catchment, it
230 was indicated that stormwater flooding occurs for $C = 2, 3, 5$ and rainfall duration $t_r = 120$ min (Szeląg et al., 2021). The
231 computed values of specific flood volume (the upper limit of 95% confidence interval) are $\kappa = 45$ $\text{m}^3 \cdot \text{ha}^{-1}$. Analyzing of the
232 rainfall data, it was observed that the number of rainfall events with depths of $P_t = 5.2\text{--}42$ mm ranged from 12 to 30 in each
233 year (210 rainfall events altogether), while the rainfall durations were between $t_r = 15\text{--}120$ min.

234

235 3.3.2. Hydrodynamic catchment model (module 2)

236 Stormwater flooding volume calculations were performed with the SWMM model using the „Flooding" function
237 (Szeląg et al. 2021). Based on the results of $Q(t)$ for j – manholes ($j = 1, 2, 3 \dots, k$) in the sub-catchments (J, K, L, M, N, O,
238 P, R, S), the total flooding volume $V_j = \int Q(t)dt$ was determined, which allowed specific flood volume (κ) values to be
239 determined from Equation (1).

240 The model of analysed catchment covers 62 ha and is divided into 92 sub-catchments with areas varying from 0.12
241 to 2.10 ha and impervious areas ranging 5 to 95%. The model comprises 82 nodes and 72 sections of channels. At the
242 calibration stage method of the „trial and error", the mean retention of the catchment equal of 4.60 mm. The Manning
243 coefficient of impervious areas was found to be $0.025 \text{ m}^{-1/3} \cdot \text{s}$ and $0.10 \text{ m}^{-1/3} \cdot \text{s}$ for pervious areas. The flow path width was
244 determined using the formula $W = \alpha \cdot A^{0.50}$, where: $\alpha = 1.35$. Catchment model calibration performed by Szeląg et al. (2021)
245 indicated that for 6 rainfall-runoff events, a very good fit of modelling outflow hydrographs to measurement results was
246 obtained (Nash - Sutcliffe coefficient was 0.85 - 0.98, coefficient of determination was equal to 0.85 - 0.99, hydrograph volumes
247 and maximum flows did not exceed 5% compared to measurement data).

248

249 3.3.3. Uncertainty analysis – GLUE (module 3)

250 In the GLUE method, the identification of model parameters was considered as a probabilistic task due to the large
251 number of parameters characterizing processes occurring in urban catchments (runoff, infiltration, flow in stormwater conduits,
252 flooding) – Szeląg et al. (2021), Kiczko et al. (2018), Mannina et al. (2018). The identification of model parameters in the
253 GLUE method depends on the transformation of an *a priori distribution* to an *a posteriori distribution* by means of a likelihood
254 function $L(Q/\theta)$, which determines the probability of a combination of parameters depending on the quality of fit of the

255 calculation result to the measured values. Uniform distribution of SWMM parameters was assumed (Table S1). Mathematical
 256 models used for description of surface runoff usually do not include runoff distribution and at most they include the range of
 257 admissible values of parameters resulting from their physical interpretation (Dotto et al., 2014; Knighton et al., 2016).
 258 Identification of distributions *a posteriori* and determination of likelihood functions the rainfall - runoff episodes 30 May 2010
 259 and 8 July 2011 were used, while for verification the episodes from 15 September 2010 and 30 July 2010 were applied. Subsequent
 260 computation steps of GLUE analysis were discussed in detail in Supplementary Information (Section 1).

261

262 3.3.4. Simulation of stormwater network operating with regards to uncertainty (module 4)

263 Based on the results of GLUE (*a posteriori* distribution SWMM parameters, 5000 sampling), the computation of
 264 stormwater network was performed for separate 175 independent rainfall events and 9 subcatchments; 35 events were used to
 265 validate the model. The values of specific flood volume for sub-catchments (J, K, L, M, N, O, P, R, S) were calculated and
 266 zero-one variables were established to develop logistic regression model. For computed values of specific flood volume ($\kappa \geq$
 267 $13 \text{ m}^3 \cdot \text{ha}^{-1}$) the variable value was denoted as 1, while in the opposite case it was 0 (Siekmann and Pinekamp, 2011).

268

269 3.3.5. Developing a logistic regression model – simulator specific flood volume (module 5)

270 Logistic regression model (LRM) is a tool used for classification. This model has been already applied for modelling
 271 stormwater flooding (Szelağ et al., 2020), identifying stormwater flooding from manholes (Jato – Espino et al., 2018) and the
 272 technical condition of sewage systems (Salman and Salem, 2012). The logistic regression model is described by the following
 273 equation:

$$274 \quad p_m = \frac{\exp(\alpha_0 + \alpha_1 \cdot x_1 + \alpha_2 \cdot x_2 + \alpha_3 \cdot x_3 + \dots + \alpha_i \cdot x_i)}{1 + \exp(\alpha_0 + \alpha_1 \cdot x_1 + \alpha_2 \cdot x_2 + \alpha_3 \cdot x_3 + \dots + \alpha_i \cdot x_i)} = \frac{\exp(X)}{1 + \exp(X)} = \frac{\exp(x_{rain} + X_{SWMM} + X_{Catchm})}{1 + \exp(x_{rain} + X_{SWMM} + X_{Catchm})} \quad (2)$$

275 where p_m – probability of a specific flood volume (understood as the need to corrective actions the stormwater network); α_0 –
 276 absolute term; $\alpha_1, \alpha_2, \alpha_3, \alpha_i$ – values of coefficients estimated with the maximum likelihood method, X – vector describing the
 277 linear combination of the independent variables; $X_{rain}/ X_{SWMM}/ X_{Catchm}$ – vector describing linear combination of statistically
 278 significant:

279 (a) rainfall characteristics ($X_{rain} = \sum_{s=1}^t \alpha_s \cdot x_s$),

280 (b) SWMM parameters ($X_{SWMM} = \sum_{k=1}^m \alpha_k \cdot x_k$),

281 (c) catchment characteristics, and stormwater network characteristics confidence level – 0.05 ($X_{Catchm} = \sum_{p=1}^r \alpha_p \cdot x_p$); x_i –
 282 independent variables describing rainfall characteristics, e.g., rainfall depth, its duration, and the parameters calibrated in the
 283 SWMM, catchment characteristics (permeability, terrain retention, density of stormwater network, length, slope, retention in
 284 stormwater channels etc.).

285 Independent variables in the logit model were calculated using the forward stepwise algorithm, recommended for the creation
 286 of such models. At the same time, it also ensures the elimination of correlated independent variables (Harrell 2001). The

287 estimation of the coefficients α_i in Equation (4) and thus the determination of the logistic regression model involved two stages:
 288 learning (80%) and testing (20%). Optimisation of the p_m threshold, equations for determining measures of fit between
 289 computational results and measurements was provided in Supplementary Information (Section 2). In this study, 35 independent
 290 rainfall events were assumed for model validation, for which $P_t = 6.0 - 15.0$ mm and $t_r = 30 - 120$ min. For validation of the
 291 LRM model, catchments J, O, S were selected, in which catchment (Imp, Impd) and topology network (Gk, Gkd, Jkp)
 292 characteristics were varied in the interaction scheme. At the variant generation step, combinations of two inputs were used to
 293 verify model, then values of which were changed in a three-point scheme -0.2/0/+0.2.

294

295 3.3.6. Sensitivity analysis (module 6)

296 According to literature data (Morio, 2011), despite simplifications, local sensitivity analysis is widely applied at the
 297 calibration stage and while analysing the hydrodynamic catchment models. In our study, the sensitivity coefficient was
 298 calculated from the equation (Petersen et al. 2012):

$$299 \quad S_{xi} = \frac{\partial p_m}{\partial x_i} \cdot \frac{x_i}{p_m} \quad (3)$$

300 Where, knowing that $\frac{\partial p_m}{\partial x_i} = \beta_i \cdot p_m \cdot (1 - p_m)$, after transformations, the following formula was obtained (Fatone et al. 2021):

$$301 \quad S_{xi} = \beta_i \cdot x_i \cdot (1 - p_m) \quad (4)$$

302 Value of the S_{xi} was calculated for calibrated SWMM parameters (Table S1), at the same time analysing the impact of rainfall
 303 duration ($t_r = 30 - 90$ min) for rainfall depth $P_t = 10$ mm (representative value for analysing stormwater network functioning
 304 according to DWA – A 118, corresponding to a heavy rainfall event). For the above assumptions, S_{xi} was determined for
 305 different catchment characteristics, which at the same time helped to evaluate the interactions between rainfall data and the
 306 parameter SWMM.

307 The probability of the specific flood volume (p_m) was computed using the logistic regression model for the sub –
 308 catchment characteristics defined in Table 2 and SWMM parameters established during calibration (Szeląg et al., 2016) for
 309 maximum convection rainfall intensity for $t_r = 30$ min and $P_t = 9.62$ mm for Kielce (Section 4 at Supplementary Information).
 310 The calculations of Szeląg et al. (2022) proved that in the urban catchment in question there is a hydraulic overload of the
 311 stormwater system due to convective rainfall. At the same time, the sensitivity coefficients for calibrated SWMM model
 312 parameters were calculated. On this basis the spatial variability of S_{xi} for the sub-basins was determined.

313

314 3.3.7. Application of the logit model to analyse stormwater operating and catchment management (module 8)

315 If the stormwater network ceases to function properly and the threshold value of p_m is exceeded, some possible
 316 improvements were suggested, including: (a) increasing the retention depth of impervious areas, i.e. an increase of d_{imp} from
 317 2.50 mm to 3.50 mm, and at the same time raising the Manning roughness coefficient from $n_{imp} = 0.025 \text{ m}^{-1/3} \cdot \text{s}$ to $n_{imp} = 0.035$
 318 $\text{m}^{-1/3} \cdot \text{s}$, (b) an increase of hydraulic capacity by reducing the Manning roughness coefficient for stormwater channels from n_{sew}

319 = 0.018 m^{-1/3}·s to n_{sew} = 0.012 m^{-1/3}·s. In addition, the possible change of spatial development of urban catchment area was
 320 taken into consideration. Finally, combinations of the above-mentioned computation variants were analysed. When the values
 321 of independent variables (catchment characteristics) adopted for the calculations exceeded the lower/upper (e.g., for Imp =
 322 0.32 - 0.41) limit of applicability of the determined logit model, the simulation results were verified with the mechanistic
 323 model. The verification procedure consisted of three steps:

- 324 a) computation of the probability of specific flood volume for rainfall with durations in the range of t_r = 30 – 90 min to assess
- 325 stormwater network operating,
- 326 b) simulation with a calibrated hydrodynamic model for rainfall data as in step (a),
- 327 c) comparison of computation results obtained in steps (a), (b); in the event of a good fit, i.e., proper identification of specific
- 328 flood volume, the results obtained from the logit model can be accepted. Three specific corrective variants have been defined
- 329 as presented in Table S2.

330

331 3.3.8. Probability of stormwater network failure (module 9)

332 The probability of failure (Sun et al., 2012; Karamouz et al., 2013) was used to analyze the performance of the sewage
 333 network in a rainfall event. In the calculations, a failure was defined as an episode (assumed rainfall data, catchment
 334 characteristics, sewer network, SWMM parameters described by *a posteriori distribution* - GLUE results discussed in Section
 335 3.3.3) in which $\kappa \geq 13\text{m}^3 \cdot \text{ha}^{-1}$ ($p_m \geq p_{m,cr}$) is exceeded. However, the probability of failure was calculated from the equation:

$$336 \quad p_F = \frac{\sum_{j=1}^N Z_j}{N}, \text{ where: } Z_j = \begin{cases} 1; & p_m \geq p_{m,cr} \\ 0; & p_m < p_{m,cr} \end{cases} \quad (5)$$

337 where: p_m – probability of specific flood volume (exceedance of this value indicates a failure), p_F – probability of the stormwater
 338 network failure in the event of rainfall, Z_j – function describing stormwater network operation, for $Z_j = 1$ – drainage system requires
 339 modernisation; otherwise, i.e. $Z_j = 0$ – modernisation is not necessary.

340 Based on Equation (5) for the assumed characteristics (rainfall, catchment, drainage network), the operating conditions of the
 341 stormwater network were determined. Hence, an algorithm is given to calculate the performance improvement of a sewer network
 342 in the context of failure probability (p_F) reduction. The above effect was obtained by introducing thresholds of maximum permissible
 343 values of Manning roughness coefficients of sewers n_{sew(m)}. It was assumed that if the value of n_{sew} (the value from the *a posteriori*
 344 *distribution*) exceeds the maximum permissible value - n_{sew(m)} and determines the occurrence of failure ($Z_j = 1$) and the need to
 345 modernize the sewers, it should be corrected in such a way that $p_m < p_{m,cr}$. The above calculations were reduced to the following
 346 steps:

- 347 a) *a posteriori distribution* of calibrated SWMM model parameters (N = 5000 samples),
- 348 b) computation of probability of specific flood volume for N items and establishment of failure probability,
- 349 c) computation of the Manning roughness coefficient for channels when $p_m > p_{m,cr}$ from the following formula:

$$n_{sew} = \frac{1}{\alpha_{n_{sew}}} \cdot \left[\ln \left(\frac{p_{m,cr}}{1-p_{m,cr}} \right) - \left(\sum_{k=1}^{m-1} \alpha_k \cdot x_k \right) - X_{rain} - X_{catchm} \right] \quad (6)$$

351 where: $k = 1, 2, 3, \dots, m$ – calibrated SWMM model parameters; $k = 1, 2, 3, \dots, m$; $\alpha_{n_{sew}}$ – estimated coefficient in logistic regression
 352 model for the Manning roughness coefficient for channels (derivation of the Equation 6 was presented in the Supplementary
 353 Information – Section 4),

354 d) establishment of empirical distribution describing the n_{sew} values calculated from Equation (6),

355 e) computation of n_{sew} values from Equation (8) for $n_{sew(un)} \leq n_{sew(m)}$ (where: $n_{sew(un)}$ – Manning roughness coefficients of channels
 356 computed in step (a), $n_{sew(m)}$ – maximal boundary (threshold) value of Manning roughness coefficient for channels), when $n_{sew(un)} \geq$
 357 $n_{sew(m)}$ to $n_{sew} = n_{sew(un)}$,

358 f) computation of probability of specific flood volume and probability of failure (p_F),

359 g) determination of empirical distribution (CDF) for n_{sew} ,

360 h) steps e – g are repeated $r = 1, 2, 3, \dots, z$ – for different values of $n_{sew,max}$ and median values of $n_{sew(0.5)} = f(n_{sew(m)}, r)$ are denoted based
 361 on empirical distributions,

362 i) steps a–h are conducted for different catchment characteristics,

363 j) graph $p_F = f(n_{sew(0.5)})$ is drawn.

364

365 4. Results

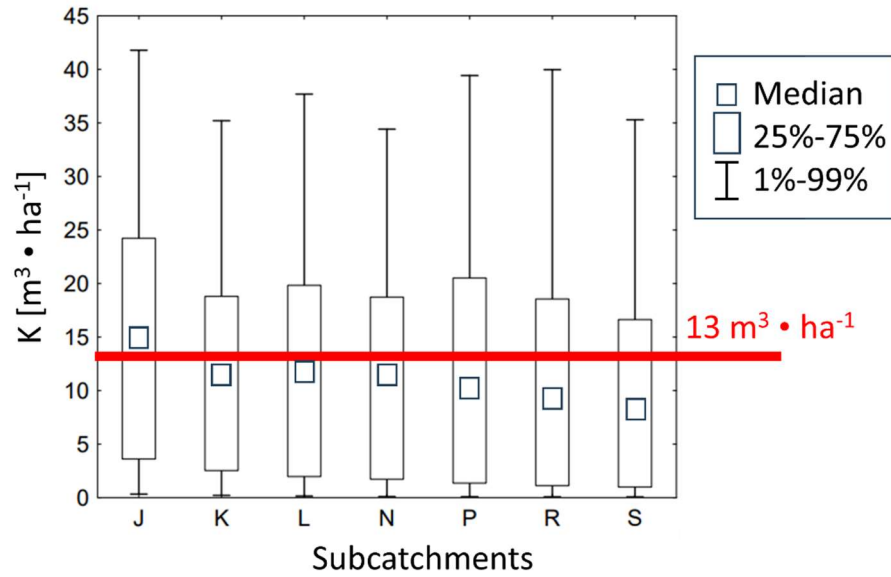
366 4.1. Uncertainty analysis – GLUE (module 3)

367 Based on SWMM simulation results including uncertainty of calibrated parameters (Table S1), the likelihood functions
 368 were determined (Kiczko et al., 2018). For the observational events (30 May 2010 and 8 July 2011) used to identify the SWMM
 369 parameters, it was found that 96% of the measurement points included the calculated confidence interval. For the validation sets,
 370 90% of the observation points fall within the bands for the 15 September 2010 event and 70% for 30 July 2010 (Figure S1). The
 371 results of the likelihood function calculations for the calibrated SWMM model parameters are given in Figures S2 – S3 in
 372 Supplementary Information.

373

374 4.2. Simulations of stormwater network operation with regard to uncertainty (module 4)

375 The results of variation of specific flood volume for the separated sub-catchments has been presented in Figure 3. Based on
 376 the obtained curves it was stated that the uncertainty of SWMM parameters influenced the simulation results, which was confirmed
 377 by the great variability of the 1% and 99% percentile values for each sub-catchment. The median values, enabled to identify that the
 378 largest specific flood volume was for sub-catchment J ($14.90 \text{ m}^3 \cdot \text{ha}^{-1}$), and $8.29 \text{ m}^3 \cdot \text{ha}^{-1}$ for the sub-catchment S (Figure 3). The
 379 simulation results for the 1% percentiles showed that for adopted rainfall events ($P_t > 5.0 \text{ mm}$ and $t_r < 150 \text{ min}$) stormwater flooding
 380 occurred in all sub-catchments.



381
382 **Figure 3. Variability of specific flood volume for sub-catchments.**

383
384 It was demonstrated that problems with operating of the stormwater network are present in each sub-catchment, since the calculated
385 values of percentiles (75%, 99%) are higher than $13 \text{ m}^3 \cdot \text{ha}^{-1}$. This indicates that the stormwater network requires modernisation.

386
387 **4.3. Determination of the logistic regression model (module 5)**

388 A LRM was built based on the operational simulation of the stormwater network. The model can be used to identify specific
389 flood volume and for decision-making regarding corrective actions of the stormwater system. The relationship from Equation (2)
390 was described by the following linear combination:

391
$$X_{rain} = 4.05 \cdot P_{tot} - 0.18 \cdot t_r - 54.15 \quad (7)$$

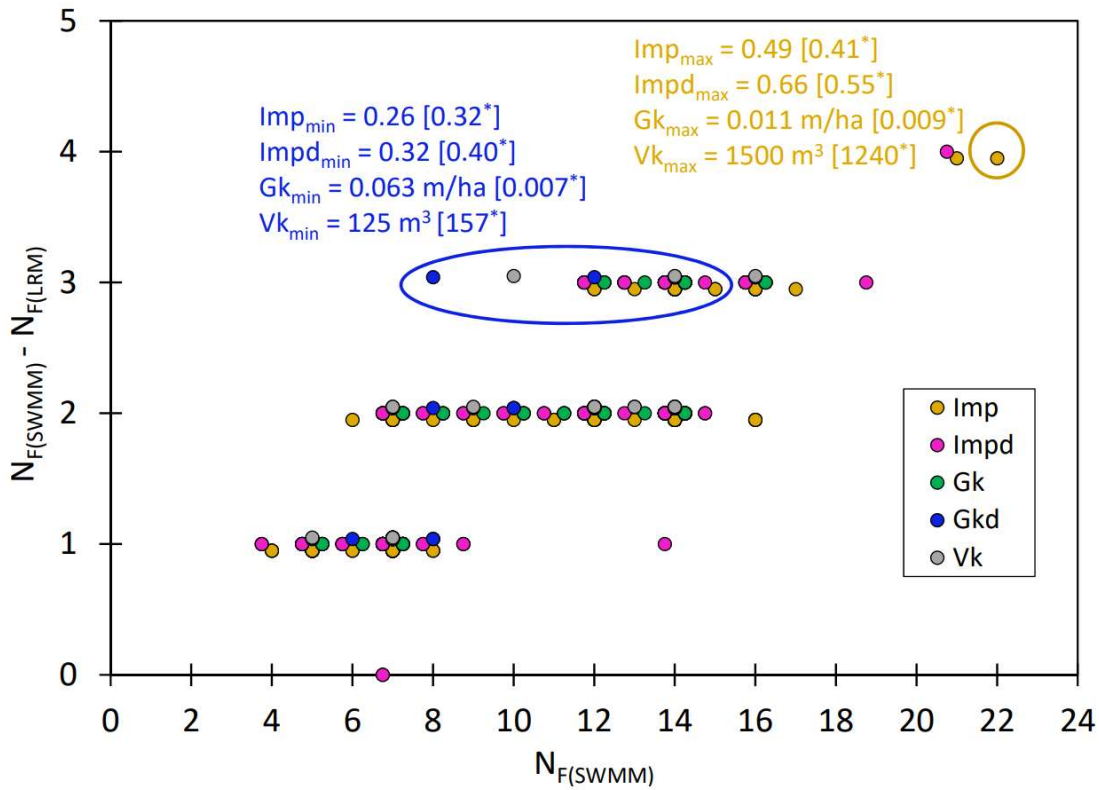
392
$$X_{SWMM} = 0.23 \cdot \alpha - 79.40 \cdot n_{imp} + 6.23 \cdot \beta + 0.33 \cdot \gamma + 234.12 \cdot n_{sew} \quad (8)$$

393
$$X_{Catch} = 76.72 \cdot Imp + 40.77 \cdot Impd - 0.01 \cdot Vk - 1967.04 \cdot Gk - 1169.00 \cdot Gkd - 20.33 \cdot Jkp \quad (9)$$

394 For other independent variables (Table S2) the determined coefficients were statistically insignificant in prediction confidence band
395 0.05. Standard deviations of the coefficients estimated from the logit model and the test probabilities are presented in Table S2. The
396 best fit of the computed results to the measurement data was obtained for $p_{m,cr} = 0.75$. For the test data set (20%) the following values
397 were obtained: SPEC = 95.24%, SENS = 84.62% and Acc = 87.87%.

398 For the determined independent variables (Equation 7, 8), calculations were performed with the LRM and SWMM model
399 (for 35 rainfall events, $P_t \geq 5 \text{ mm}$ and $t_r \leq 120 \text{ min}$) assuming values of catchment characteristics and topological data within ± 0.2 in
400 the separated sub-catchments. The results of the validation of the developed model for the identification of the specific flood
401 volume are given in Tables S5 - S11. The results obtained confirm that the determined LRM model can be applied in a wider range

402 than shown in Table 1. In the range of $N_{F(SWMM)} = (0 - 6)$, the relative difference in the number of episodes when $\kappa \geq 13 \text{ m}^3 \cdot \text{ha}^{-1}$
 403 did not exceed 20%, and for $N_{F(SWMM)} = <6, 19>$ was 15 - 33% (Figure 4).

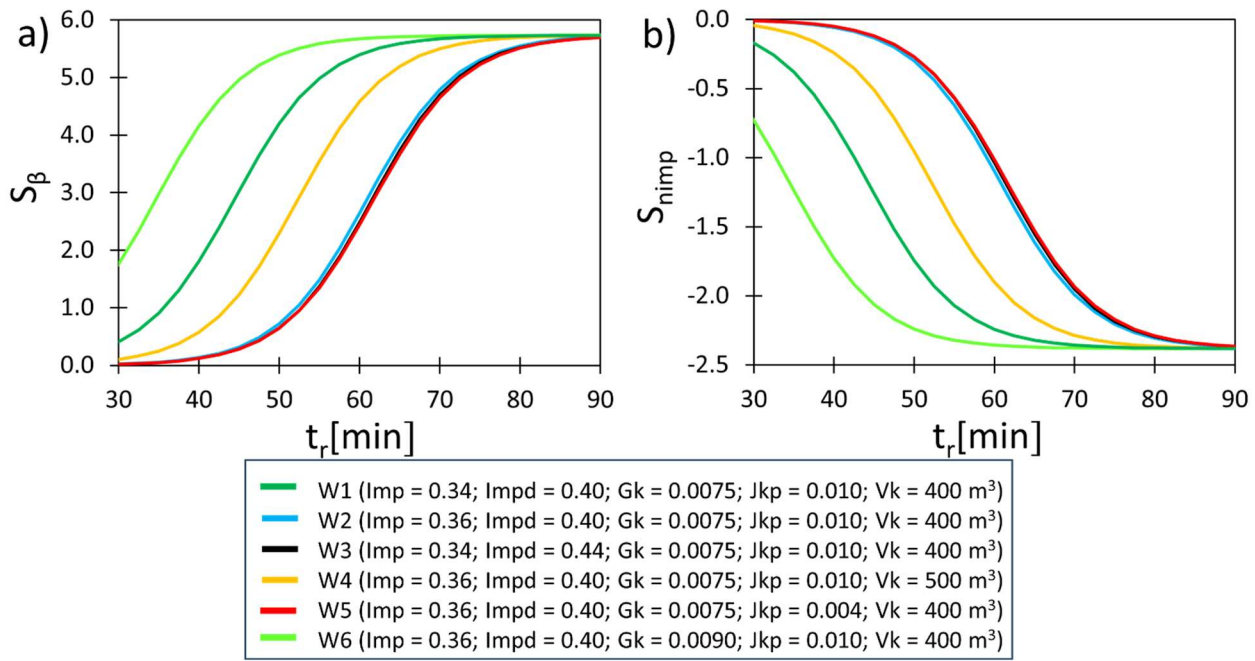


404
 405 **Figure 4.** Comparison of LRM and SWMM simulation results of the number of episodes when the specific flood volume
 406 was greater than $13 \text{ m}^3 \cdot \text{ha}^{-1}$ (where: $N_{F(SWMM)}$ – prediction of SWMM, $N_{F(LRM)}$ – prediction of LRM; * - minimum, maximum
 407 values of the catchment characteristics, topology of the stormwater network in Table 1; yellow - the upper limit of the model,
 408 blue - the lower limit of the model).
 409

410 The maximum difference between LRM and SWMM simulations ($N_{F(SWMM)} - N_{F(LRM)} = 4$) was obtained for $Imp = 0.49$, $Impd$
 411 $= 0.66$, $Gk = 0.011 \text{ m-ha}^{-1}$, $Vk = 1500 \text{ m}^3$, which corresponds to the extreme values of the catchment characteristics, the
 412 topology of the sewer network. Verification results showed that the maximum difference in the number of events when $\kappa > 13$
 413 $\text{m}^3 \cdot \text{ha}^{-1}$ by the ML model and SWMM for $Imp = 0.26 - 0.50$, $Impd = 0.32 - 0.66$, $Gk = 0.0068 - 0.011 \text{ m}^3 \cdot \text{ha}^{-1}$, $Gkd = 0.0009 -$
 414 $0.0013 \text{ m}^3 \cdot \text{ha}^{-1}$ did not exceed 4 episodes (Figure 4). The calculations performed confirm the high fitting of the calculations with
 415 measurements of the number of episodes when the specific flood volume exceeds $13 \text{ m}^3 \cdot \text{ha}^{-1}$.
 416

417 4.4. Sensitivity analyses (module 6)

418 For rainfall depth $P_{tot} = 10 \text{ mm}$ and duration $t_t = 30 - 90 \text{ min}$, the sensitivity coefficients for the SWMM model were
 419 determined, based on Equation (4). For calculation of S_{xi} the values established during calibration were adopted (Kiczko et al., 2018).
 420 The computation results for two parameters of the SWMM model (β and n_{imp}) are presented in Figure 5.



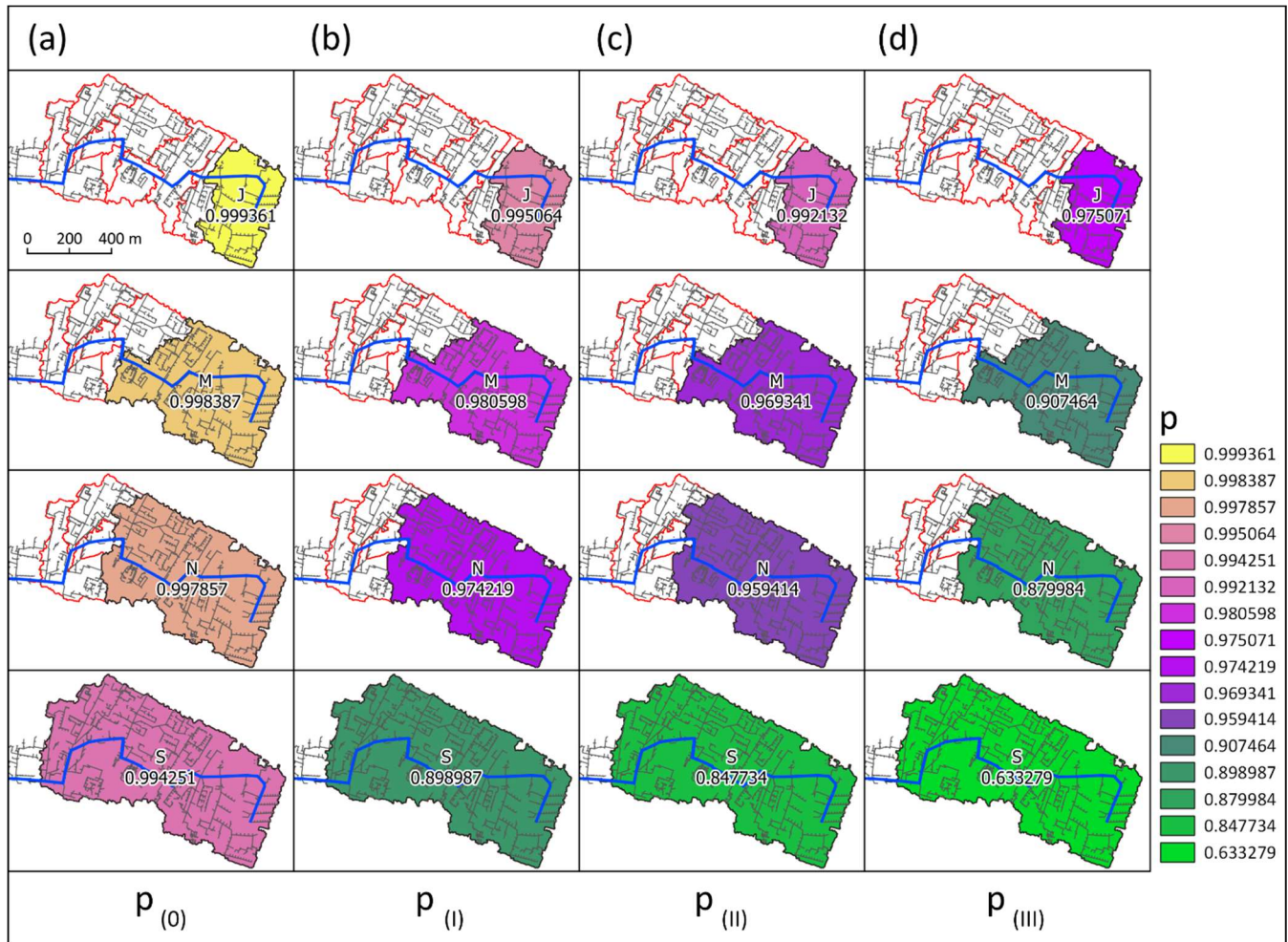
421

422 **Figure 5. The impact of rainfall duration (t_r) and catchment characteristics (Imp, Impd, Vk, Jkp) on sensitivity coefficients:**
 423 **(a) S_β , (b) S_{nimp} .**
 424

425 These two parameters appeared to have the most significant impact on specific flood volume and, at the same time, they present a
 426 vastly different impact on the dynamics of changes regarding $S_{xi} = f(t_r, Imp, Impd, Vk, Jkp)$; the calculation results for the other
 427 SWMM model parameters are given in Figures S4–S8 (Supplementary Information). The Figure 5 and Figures S4 – S8 indicated
 428 that for the adopted values of t_r and Imp, Impd, Vk, Jkp, the highest values of S_{xi} was obtained for correction coefficient percentage
 429 of impervious areas (β), Manning roughness coefficient for sewer channels (n_{sew}) and Manning roughness coefficient for
 430 impervious areas (n_{imp}). Retention depth of impervious areas (d_{imp}) had the lowest impact on the results of specific flood
 431 volume. An increase of rainfall duration results in higher values of S_β , S_{nimp} (Figure 5). The lowest sensitivity coefficients
 432 were obtained for $t_r = 30$ min while the highest for $t_r = 90$ min. An increase of Imp, Impd results in a decrease of S_β and S_{nimp}
 433 sensitivity coefficients. For instance, an increase of Imp from 0.34 to 0.36 results in a decrease of S_β from 1.23 to 0.28; identical
 434 values were obtained for Impd (Figure 5). Moreover, an increase of Vk, Jkp, Gk leads to an increase of S_β and S_{nimp} sensitivity
 435 coefficients. Among analysed catchment characteristics, density of stormwater network (Gk) had the highest impact on
 436 sensitivity coefficients, while longitudinal slope of canal (Jkp) was of the lowest significance, which is confirmed by variability
 437 of obtained curves for subsequent SWMM parameters (Figure 5). For example, when Vk increased from 400m³ to 500 m³, S_β
 438 increased from 0.29 to 0.82. Additionally, a 10% growth of S_β was observed due to a change of $Jkp = 0.004$ to $Jkp = 0.010$.
 439 Finally, when Gk increased from 0.0075 to 0.009 S_β also increased from 0.29 to 3.03 (Figure 5).

440 **4.6. Implementation of logit model to analyse the operating of the stormwater network and catchment management**
 441 **(module 7 & 8)**

442 Due to the fact that in the analysed stormwater network an exceedance of specific flood volume was observed,
 443 possible improvements to the network were considered in terms of correcting catchment imperviousness (Imp) as well as
 444 enhanced terrain retention and channel capacity. The results of p_m computations are presented in Figure 6, while Figure 7
 445 shows S_β for variants I, II and III for sub-catchments.



446
 447 **Figure 6. Probability of specific flood volume in sub-catchments for: (a) present state (p_0) and for (b) I, (c) II, (d) III**
 448 **corrective actions variants.**

449 Simulation results for the sensitivity coefficients of other SWMM model parameters (Table S1) and the probability of specific
 450 flood volumes are presented in Figures. S9–S17. A decrease of Imp by 10% in sub-catchment J has negligible impact on p_m
 451 value, while in sub-catchment S it results in the decrease of specific flood volume probability by 10% (Figure 6a, 6b). It was
 452 found that decrease of catchment imperviousness (variant I) leads to improvement of stormwater system operation (Figure 6).

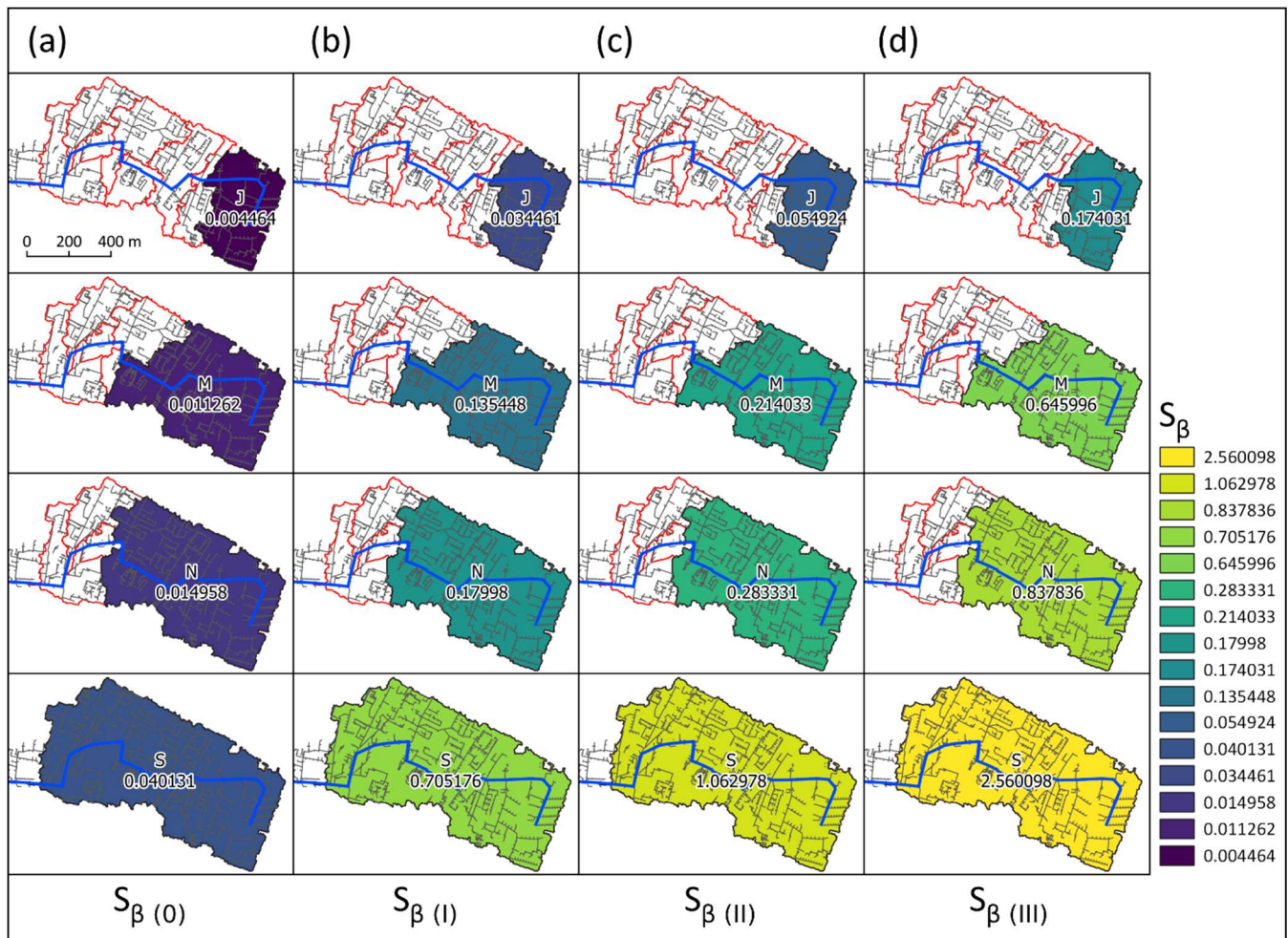


Figure 7. Sensitivity coefficient (S_{β}) in sub-catchments for: (a) present state (0) and for (b) I, (c) II, (d) III corrective action variants.

453

454

455

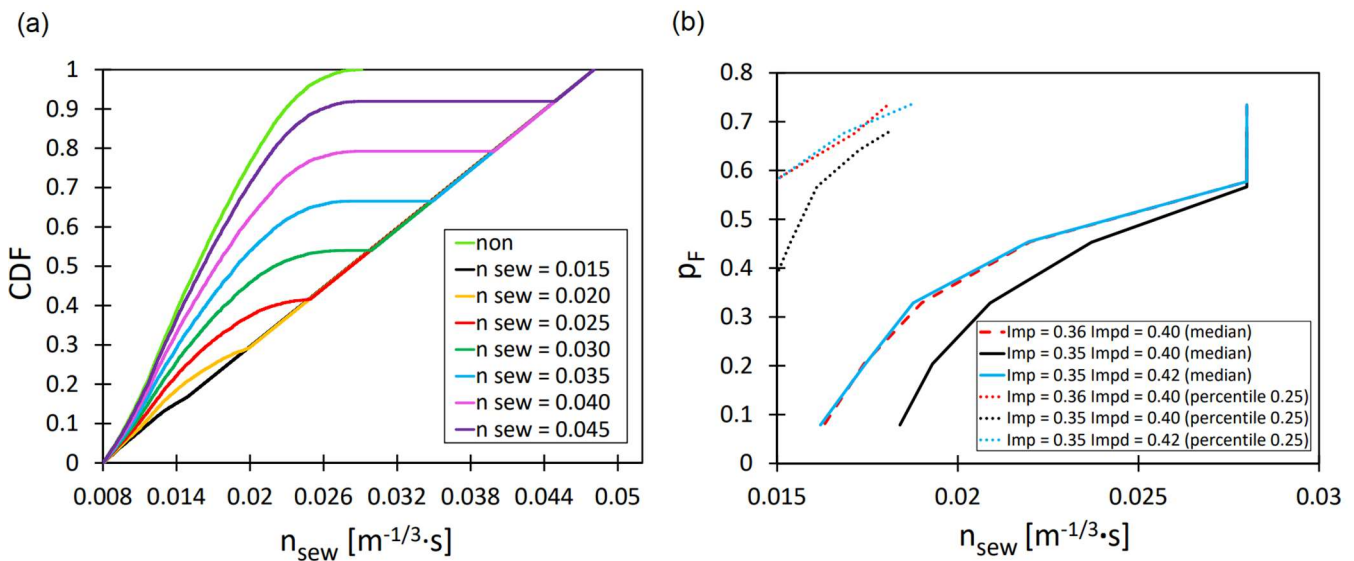
456

457 The greatest reduction in volume flooding was obtained for variant III, when p_m values decreased by 2% and 36% for sub-
 458 catchments J and S (Figure 6d). Based on the p_m values in catchments J, M, N, S for corrective action variant III, it was found
 459 that, despite the increase in retention depth, channel capacity and reduction in imperviousness of the catchments, there was
 460 hydraulic overloading ($\kappa > 13 \text{ m}^3 \cdot \text{ha}^{-1}$) in the sub-catchments. This indicates the need for further changes to both the catchment
 461 and the stormwater network than was assumed. For variants I, III the Imp values for the sub-catchment are below the
 462 applicability range of the logit model, so mechanistic model simulations were performed to verify the results (Table S4). The
 463 results of the model calculations confirm their high agreement; out of 72 cases, identical results were obtained in 68 cases. The
 464 calculations performed (variant I, II, III) for the sub-catchment showed a greater influence of changes in terrain retention and
 465 channel capacity on the sensitivity coefficients than the probability of specific flood volume (Figure 7). For catchments J, S, a
 466 10% decrease in Imp (variant I) increased S_{β} by 7.55 times and 17.50 times (Figure 7a, 7d). For variant II (increasing catchment

467 retention), sensitivity coefficients were found to be higher than 51% (catchment S) and 59% (catchment J) compared to variant
 468 I, and the highest S_{β} was obtained in variant III. The S_{β} values for sub-catchment S are higher than in catchment J by 20.7
 469 times, 19.3 times and 14.7 times for variants I, II and III, respectively. These results provide relevant information for planning
 470 retention infrastructure that reduces outflow.

471
 472 **4.7. Probability of failure (module 9)**

473 Based on SWMM model parameters determined via the MCM method (Table S1), probability of failure (p_F) was
 474 computed for convection rainfall in Kielce with a duration time of $t_r=30$ min and $P_{tot}=9.61$ mm. The following threshold values
 475 of $n_{sew(m)}$ were adopted for calculations: $n_{sew(m)} = 0.015 - 0.045 \text{ m}^{-1/3} \cdot \text{s}$, coupled with three variants of catchment characteristics:
 476 $Imp = 0.36$ and $Impd = 0.40$; $Imp = 0.35$ and $Impd = 0.40$; $Imp = 0.35$ and $Impd = 0.42$. The impact of canal retention ($V_k =$
 477 $750, 850, 950 \text{ m}^3$); density of stormwater network ($G_k = 0.0075, 0.0080, 0.0085 \text{ m} \cdot \text{ha}^{-1}$; $G_{kd} = 0.005, 0.006, 0.007 \text{ m} \cdot \text{ha}^{-1}$) in
 478 upper and lower part of the catchment on probability of failure (p_F) was also analysed. The Manning roughness coefficients of
 479 the channels (n_{sew}) for the analysed variants were presented as empirical distribution (CDF). In Figure 8a, 9a the results for
 480 $Imp = 0.36, Impd = 0.40$ and $V_k = 750, 850, 950 \text{ m}^3$ are presented, while other variants are shown in Figures S18, S19.
 481

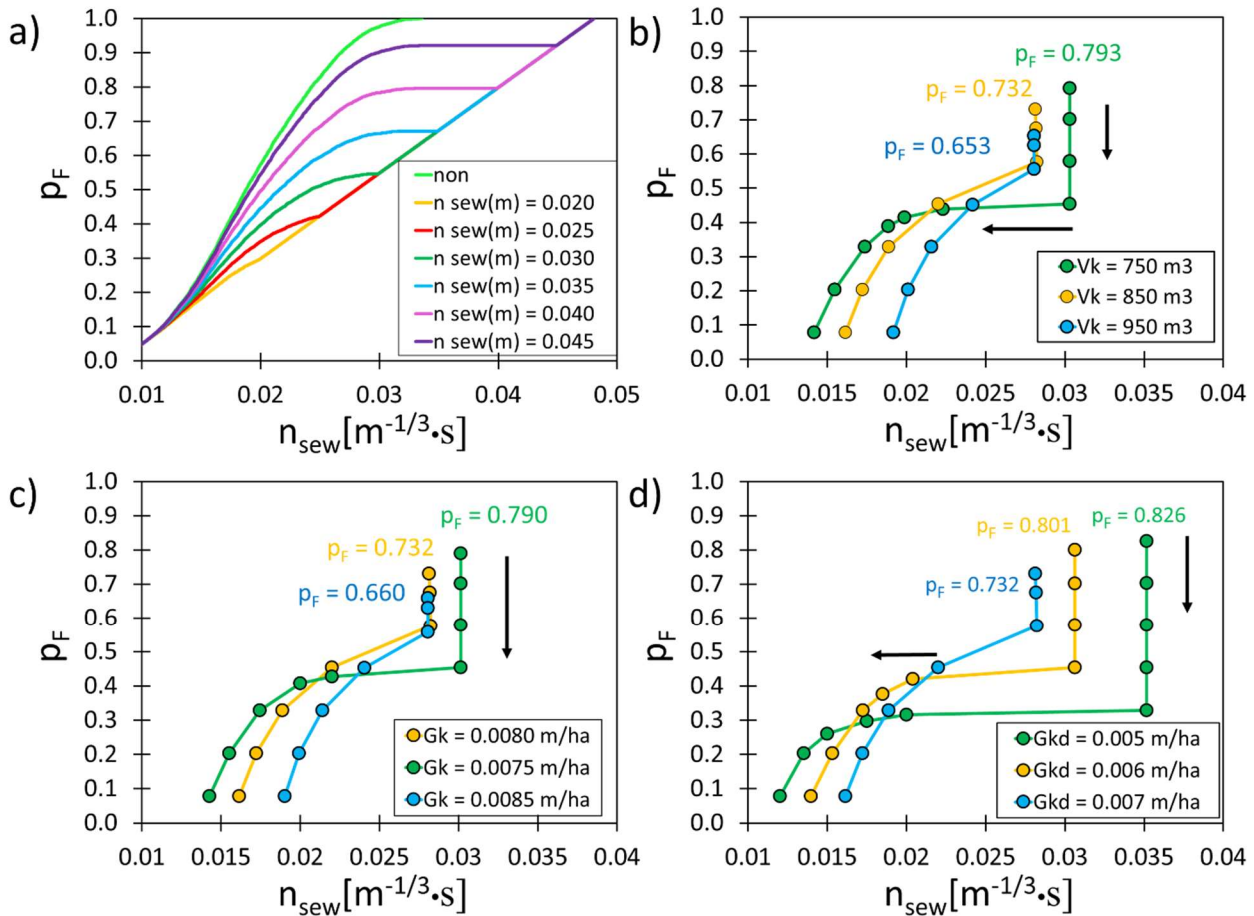


482
 483 **Figure 8. (a) Empirical distributions of threshold values of Manning roughness coefficients of channel (n_{sew}). (b) Impact**
 484 **of Manning roughness coefficient of channel on failure probability (p_F) in relation to $Imp, Impd$.**
 485

486 Figure 8b presents the impact of $n_{sew}=f(n_{sew(m)})$ for percentiles 0.25 and 0.50 (based on the curves in Figures 8b, 9b, 9c, 9d,
 487 S25, S26 the values of the respective percentiles for the analysed $n_{sew(m)}$) on the probability of failure (p_F). Assuming that
 488 Manning roughness coefficients – $n_{sew(un)}$ determined by MC simulation which exceeds the threshold triggers the corrective
 489 actions of sewer pipes resulting in reduction of roughness below $n_{sew(m)}$ following the condition in which the stormwater
 490 network functions $p_m = f(X_{rain}, X_{SWMM}, X_{ctchm}) > 0.75$ for an independent rainfall event, it was found out, that an

491 appropriate decrease of percentiles (0.25 and 0.50 - median) leads to improved network operation and to a lower failure
 492 probability (Figures. 8a, 8b). It was observed that the change of percentile 0.50 for n_{sew} for a sample from MC simulation leads
 493 to a decrease from $0.028 \text{ m}^{-1/3} \cdot \text{s}$ to $0.021 \text{ m}^{-1/3} \cdot \text{s}$ (as a result of correction $n_{sew(un)} < n_{sew(m)}$) and to improved stormwater network
 494 operation understood as a lower probability of failure (decrease of p_F from 0.68 to 0.42 for $Imp = 0.36$ and $Impd = 0.40$). These
 495 results confirm the significance of catchment characteristics (Imp , $Impd$) for the operability of a stormwater network. For $Impd$
 496 = 0.40, the reduction in catchment impervious area (Imp) from 0.36 to 0.35, at percentile $n_{sew} = 0.019 \text{ m}^{-1/3} \cdot \text{s}$ results in a
 497 decrease in failure probability from $p_F = 0.42$ to $p_F = 0.33$ (Figure 8b).

498 Great impact of channel retention (V_k) and density of stormwater network in the upper and lower part of a catchment
 499 (G_{kd} and G_k , respectively) on probability of failure p_F were indicated (Figure 9). For $n_{sew} < 0.0215 \text{ m}^{-1/3} \cdot \text{s}$ p_F reached higher
 500 values (max. 0.41) than for $V_k = 850 \text{ m}^3$ and $V_k = 950 \text{ m}^3$.



501
 502 **Figure 9. (a) Empirical distributions of threshold values of Manning roughness coefficients of channels (n_{sew}) for**
 503 **$V_k = 950 \text{ m}^3$. Impact of Manning roughness coefficient for channel on failure probability (p_F) in relation to: (b) V_k -**
 504 **canal retention, (c) G_k - length of stormwater channel per impervious area in a catchment ($\text{m} \cdot \text{ha}^{-1}$), (d) G_{kd} - length of**
 505 **a channel per impervious area below closing cross-section ($\text{m} \cdot \text{ha}^{-1}$).**

506 The highest failure probability ($p_F = 0.80$) was obtained for $V_k = 750 \text{ m}^3$ ($n_{\text{sew}} = 0.031 \text{ m}^{-1/3} \cdot \text{s}$), while the lowest $p_F = 0.65$ was
 507 obtained for $V_k = 950 \text{ m}^3$ (Figure 9b). Furthermore, the highest probability of failure $p_F = 0.79$ was obtained for $G_k = 0.0075$
 508 $\text{m} \cdot \text{ha}^{-1}$ ($n_{\text{sew}} = 0.031 \text{ m}^{-1/3} \cdot \text{s}$), while the lowest for $G_k = 0.0085 \text{ m} \cdot \text{ha}^{-1}$ ($n_{\text{sew}} = 0.0276 \text{ m}^{-1/3} \cdot \text{s}$) (Figure 9c). It was established
 509 that for $n_{\text{sew}} < 0.023 \text{ m}^{-1/3} \cdot \text{s}$ computed values of p_F for $G_k = 0.0075 \text{ m} \cdot \text{ha}^{-1}$ and $G_k = 0.0080 \text{ m} \cdot \text{ha}^{-1}$ are higher than 0.41.
 510 Moreover, the highest failure probability p_F for $n_{\text{sew}} = 0.035 \text{ m}^{-1/3} \cdot \text{s}$ was equal to 0.82 for $G_{kd} = 0.005 \text{ m} \cdot \text{ha}^{-1}$, while for $G_{kd} =$
 511 $0.007 \text{ m} \cdot \text{ha}^{-1}$ it was 0.73 (Figure 9d).

512

513 5. Discussion

514 Developing and calibrating mathematical models to simulate stormwater network operation under hydraulic overloads
 515 is one of the latest areas of research. In comparison to the models used so far (Li and Willems, 2019; Thorndahl 2009), the
 516 logistic regression model proposed in this study includes SWMM model parameters describing catchment retention and, at the
 517 same time, the characteristics of the catchment and stormwater network (Table 4).

518

519 **Table 4. Comparison of developed model for identification of specific flood volume to literature data**

Study	Criteria	M	I	R	C	S	P
Duncan et al. (2011)	occurrence of flooding	✓	•	✓	✓	✓	•
Jato - Espino et al. (2018)	occurrence of flooding	✓	✓	✓	✓	✓	•
Jato - Espino et al. (2019)	occurrence of flooding	✓	•	✓	✓	✓	•
Li and Willems (2020)	occurrence flooding	✓	✓	✓	✓	✓	•
Szeląg et al. (2021)	volume	✓	✓	✓	✓	✓	✓
Szeląg et al. (2022a)	occurrence of flooding	•	•	✓	✓	✓	✓
Szeląg et al. (2022b)	specific flood volume	✓	✓	✓	•	•	✓
Thorndahl et al. (2008)	volume	✓	✓	✓	•	✓	✓
Verbovski et al. (2022)	volume	✓	✓	✓	•	•	•
Fu et al. (2011)	volume	•	•	✓	✓	✓	✓
Chen et al. (2020)	volume	•	•	✓	✓	✓	✓
Fraga et al. (2016)	volume	•	•	✓	✓	✓	✓
this study	specific flood volume	✓	✓	✓	✓	✓	✓

520

521 where: M (method); the models were divided into two groups: mechanistic (•) and statistical model (✓); R (rainfall); C
 522 (catchment); S (sewer); P (calibration parameter); I (interpretation model, based on estimated factors the impact of analysed
 523 factors on stormwater flooding can be determined).

524

525 Apart from the model developed in this study, the above-mentioned factors are only included in MCM, which have a form of
 526 differential equations. Therefore, they require a large number of simulations in order to determine the impact of selected
 527 variables on computation results of specific flood volume. Free from such drawbacks are statistical models (Table S4) that

528 take the form of empirical relationships. For models developed with neural networks, there is a need of performing additional
529 analyses (Ke et al, 2020; Yang et al., 2020). Jato – Espino et al. (2018, 2019) and Li and Willems (2020) analysed stormwater
530 flooding from manholes based on catchment characteristics and stormwater network characteristics (Table 4). Szeląg et al.
531 (2022) confirmed their results and developed a model for identification of stormwater flooding in a catchment, but not
532 considered catchment retention. In this context, the approaches cited above were insufficient to analyse the impact of different
533 types of pavement (for example roof, road, parking etc.) on sewage flooding. Fu et al. (2011), Thorndahl et al. (2009), Szeląg
534 et al. (2022b) analysed the uncertainty of the identified parameters, which allowed, for example, to correct for impervious area
535 retention, roughness coefficient without being able to correct for catchment imperviousness, which limited the use of the
536 models in catchment management. The approach proposed in this study is a combination of these two solutions, which provides
537 a tool which can be successfully implemented to manage other catchments.

538 The results of this study confirmed the major significance and huge interaction between catchment characteristics and
539 SWMM model parameters. This fact can be further compared by several references (Li and Willems, 2020; Jato – Espino et
540 al., 2019; Zhuo et al., 2019) presenting comparisons of flooding simulations in urban catchments. This analysis indicated that
541 an impervious area in a catchment (Imp, Impd) leads to the increase of flooding; reverse dependency was obtained by Jato –
542 Espino et al. (2018) when modelling flooding from manholes. Increase in channel volume above the closing cross-section of
543 a catchment (V_k) and its longitudinal slope (J_{kp}) results in the decrease of flooding, that was confirmed for Espoo catchment
544 in Finland (Jato – Espino et al. 2018). The increase of unit impervious area per the length of main stormwater interceptor (G_k ,
545 G_{kd}) results in smaller volume of stormwater flooding. This is due to the relationship that the longer the channel, the greater
546 the number of manholes. Huang et al. (2018) based on observations conducted in a complex stormwater system indicated the
547 impact of catchment location and hydrological conditions on the peak flow of flooding. Yao et al. (2019) obtained similar
548 results after computations with a MCM for catchments in Beijing and in Dresden (Reyes – Silva et al. 2020).

549 Calculation results obtained in this study confirmed relevant impact of rainfall data, catchment characteristics, and
550 stormwater network characteristics on sensitivity coefficients – relationships between SWMM parameters and specific flood
551 volume. For rainfall data and catchment characteristics (assumed as constant) it was proved that correction coefficient of
552 impervious area (β) and the Manning roughness coefficient for channels (n_{sew}) have the greatest impact on specific flood
553 volume. The results of this computations were consistent with Thorndahl et al. (2009), who simulated flooding from a single
554 manhole in the Frejlev catchment (Belgium), based on rainfall data and calibrated parameters of a MCM. These findings were
555 confirmed by calculations Fu et al. (2012) and Prodanovic et al. (2022) respectively for catchments of 400 ha and 8 ha. Szeląg
556 et al. (2021, 2022b) based on simulations with MCM including uncertainty of SWMM parameters proved the key impact of
557 Manning roughness coefficient of sewers on specific flood volume (for rainfall event $t_r = 30$ min and $P_t = 15.25$ mm). Fraga
558 et al. (2016) used GLUE+ GSA method for a road catchment and indicated the impact of rainfall data (rainfall duration, depth,
559 temporal distribution) on sensitivity analysis results. It was confirmed in computations of stormwater flooding using logit
560 model (Szeląg et al. 2022) and specific flood volume calculations with SWMM model (Freni et al. 2012). Xing et al. (2021)
561 used MCM to determine characteristics of spatial development and stormwater characteristics in Chongqing catchment (China)

562 on the depth of stormwater flooding. The aforementioned research studies indicate the impact of rainfall data, catchment
563 characteristics, and stormwater network characteristics on sensitivity of hydrodynamic simulation model for stormwater
564 flooding.

565 The sensitivity analysis development proposed in this study enabled its application for catchments with different
566 characteristics, which is an improvement compared to previously applied, more specified approaches (Cristiano et al. 2019;
567 Fatone et al., 2021). Differences in probability of occurrence/sensitivity coefficients indicate the influence of catchments
568 downstream on conditions in the catchment above. The variation in sensitivity coefficients does not account for local conditions
569 within the side channels. Due to the creation of successive sub-catchments by combining them, the conditions of the sewer
570 system in its area are averaged out, making the interpretation of the results difficult. Using the developed tool, catchment
571 management may become difficult when there is a particularly hydraulically overloaded area within the catchment, which
572 impacts neighbouring sub-catchments.

573 As in the case to the sensitivity analysis, in this study the extension of the sewer system failure assessment has been
574 adapted to enable the implementation for a random catchment (for the sewer system without pump stations). Calculations
575 outputs showed the influence of the catchment and sewage network characteristics on the failure probability. The introduction
576 of the maximum allowable value of the Manning roughness coefficient for the sewer channel, enabled to model the
577 improvement of the operating conditions of the sewage network under uncertainty. A similar approach was used in the study of
578 Fu et al. (2012) by limiting to probabilistic rainfall characteristics (Del Giudice, et al. 2013) and using a MCM to simulate the drainage
579 system. Fu et al. (2011) modified the above approach by focusing on the impact of uncertainty in the calibrated parameters on
580 flooding; however, it was not possible to analyse retention, channel capacity on system performance.

581

582 **6. Conclusions**

583 In this study a novel simulator of logistic regression extended by advanced risk assessment was developed for
584 modeling stormwater systems operation under uncertainty. The proposed model is an alternative approach to mechanistic
585 models, that can be used at the preliminary stage of analyses related to spatial planning, urban development and expansion etc.
586 This is of major significance since at the preliminary stage, the data set for building catchment models is limited and urgent
587 demand for simulation algorithm to assist decision making is required. Assuming Manning roughness coefficients – $n_{sew(un)}$
588 estimations that exceed the threshold triggers corrective actions of sewer pipes resulting in a reduction of roughness below
589 $n_{sew(m)}$ following the condition of proper functioning of the stormwater network ($p_m > p_{mcr}$). Appropriate decrease of percentiles
590 (0.25 and 0.50 - median) led to improved network operation and to a lower failure probability requirement.

591 In the adopted hydrodynamic model (based LRM), the impact of rainfall data, catchment characteristics (impervious
592 areas in the downstream and upstream) and stormwater network characteristics (the length of channel per unit impervious area,
593 channel slope and volume) as well as SWMM parameters (roughness coefficient for sewer channel, correction coefficient for
594 percentage impervious area Manning roughness coefficients for impervious area) were included simultaneously. The obtained
595 simulations results show the strong interaction between the above-listed parameters. This is extremely relevant in the context

596 of models calibration that can be applied to analyse stormwater network operation and to support the decision-making process
597 (management of stormwater in an urban catchment). Since the proposed solution analyses the spatial distribution of sensitivity
598 coefficients, it is possible to identify the most vulnerable areas inside a catchment that require specific attention while
599 identifying SWMM model parameters, which could also be taken into account when locating measuring facilities.

600

601 **7 Appendices**

602 **Appendix A: List of Symbols**

603

604 Symbols:

605 A_{pav} – area of paved surface (ha),

606 dHI – height difference of the terrain at section above closing cross-section (m),

607 dHp – height difference at section above closing cross-section (m),

608 CDF – Cumulative Distribution Function (–),

609 d_{imp} – retention depth of impervious areas (mm),

610 d_{perv} – retention depth of pervious areas (mm),

611 F – catchment surface area (ha),

612 Gk – length of stormwater channel per impervious area in a catchment ($m \cdot ha^{-1}$),

613 Gkd – length of a channel per impervious area below closing cross-section ($m \cdot ha^{-1}$),

614 $GLUE$ - Generalized Likelihood Uncertainty Estimation,

615 Hst – the height of a manhole at closing cross-section (m),

616 Imp – impervious area,

617 $Impd$ – impervious area of a catchment of downstream area,

618 J – average rainfall intensity ($l \cdot (s \cdot ha)^{-1}$),

619 Jkp – channel slope above closing cross-section of a catchment

620 K – total number of sewer manholes (–),

621 Lk – length of channel above closing cross-section of a catchment (m),

622 $L(Q/\theta)$ – likelihood function,

623 n_{imp} – Manning roughness coefficient for impervious areas ($m^{-1/3} \cdot s$),

624 n_{perv} – Manning roughness coefficient for pervious areas ($m^{-1/3} \cdot s$),

625 n_{sew} – Manning roughness coefficients of sewer channels ($m^{-1/3} \cdot s$),

626 Q_z – denote z -th value from the times series of observed and computed discharges ($m^3 \cdot s^{-1}$),

627 P_t – maximum depth of rainfall (mm),

628 p – cumulative distribution function (CDF),

629 p_m – probability of specific flood volume,

630 $P(\theta)$ – stands for *a priori* parameter distribution,
631 $R.t.$ – height difference of the channel (m),
632 S_{xi} – sensitivity coefficient,
633 x_i – independent variables,
634 *SWMM* – Storm Water Management Model,
635 t_r – duration of rainfall (min),
636 $V()$ – variance,
637 V_k – volume of stormwater channel (m^3),
638 V_{kd} – total retention of a catchment.
639 V_{kp} – volume of the channel above the closing cross-section of a catchment (m^3),
640 V_{rd} – catchment retention above the closing cross-section (m^3),
641 $V_{i(i)}$ – floodings volume from i - th sewer manhole (where: $i = 1, 2, 3, \dots, k$) (m^3),
642 W – width of the runoff path in a subcatchment (m),
643 α – Coefficient for flow path width (–),
644 β – Correction coefficient for percentage of impervious areas (–),
645 γ – Correction coefficient for subcatchment slope (–),
646 ε – a scaling factor for the variance of model residua, used to adjust the width of the confidence intervals,
647 κ – specific flood volume ($m^3 \cdot ha^{-1}$),
648

649 **Code availability:** The authors announce that there is no problem sharing the used model and codes upon request to the
650 corresponding author.
651

652 **Data availability:** The authors confirm that data supporting the findings of this study are available from the corresponding
653 author upon request.
654

655 **Author contribution:** Conceptualization: Szelałag, Methodology: Fatone, Szelałag, Kiczko; Formal analysis and investigation:
656 Szelałag, Kiczko, Stachura, Wałek; Writing - original draft preparation: Szelałag, Kowal, McGarity, Wojciechowska, Wałek,
657 Fatone, Caradot; Writing - review and editing: Kowal, Wojciechowska, McGarity, Fatone, Caradot; Supervision: Szelałag,
658 Kowal, McGarity, Wojciechowska, Caradot.
659

660 **Competing interests:** The authors declare that they have no conflicts of interest.
661

662 References

663 Babovic, F., Mijic, A., Madani, K.: Decision making under deep uncertainty for adapting urban drainage systems to change.
664 Urban Water J, 15, 552 – 560. <https://doi.org/10.1080/1573062X.2018.1529803>, 2018.
665 Ball, J., E. : An Assessment of Continuous Modeling for Robust Design Flood Estimation in Urban Environments. Front. Earth
666 Sci. 8, 1 – 10. <http://doi.org/10.3389/feart.2020.00124>, 2020.

667 Beven, K., Binley, A.: The future of distributed models: model calibration and uncertainty prediction, *Hydrol. Process.*, 6,
668 279-298, <https://doi.org/10.1002/hyp.3360060305>, 1992.

669 Bui, D.T., Hoang, N.D., Martínez-Álvarez, F., Ngo, P.T. T., Hoa, P.V., Pham, T.D., Samui, P., Costache, R.: A novel deep
670 learning neural network approach for predicting flash flood susceptibility: A case study at a high frequency tropical storm area,
671 *Sci. Total Environ*, 701, 134413. <https://doi.org/10.1016/j.scitotenv.2019.134413>, 2018.

672 Cea, L., Costabile, P.: Flood Risk in Urban Areas: Modelling, Management and Adaptation to Climate Change. A Review.
673 *Hydrology*, 9, 50. <https://doi.org/10.3390/hydrology9030050>, 2022.

674 Chang, H., Pallathadka, A., Sauer, J., Grimm, N.B., Zimmerman, R., Cheng, C., Iwaniec, D.M., Kim, Y., Lloyd, R.,
675 McPhearson, T., Rosenzweig, B., Troxler, T., Welty, C., Brenner, R., Herreros-Cantis, P.: Assessment of urban flood
676 vulnerability using the social-ecological-technological systems framework in six US cities, *Sustain. Cities Soc.* 68, 102786,
677 <https://doi.org/10.1016/j.scs.2021.102786>, 2020.

678 Chen, L., Li, S., Zhong, Y., and Shen, Z.: Improvement of model evaluation by incorporating prediction and measurement
679 uncertainty, *Hydrol. Earth Syst. Sci.*, 22, 4145–4154, <https://doi.org/10.5194/hess-22-4145-2018>, 2018.

680 Chen, W., Li, Y., Xue, W., Shahabi, H., Li, S., Hong, H., Wang, X., Bian, H., Zhang, S., Pradhan, B., Bin Ahmad, B.: Modeling
681 flood susceptibility using data-driven approaches of naïve Bayes tree, alternating decision tree, and random forest methods,
682 *Sci. Total Environ.* 701, 134979. <https://doi.org/10.1016/j.scitotenv.2019.134979>, 2019.

683 Cristiano, E., ten Veldhuis, M. C., Wright, D. B., Smith, J. A., and van de Giesen, N.: The Influence of Rainfall and Catchment
684 Critical Scales on Urban Hydrological Response Sensitivity, *Water Resour. Res.*, 55, 3375–3390,
685 <https://doi.org/10.1029/2018WR024143>, 2019.

686 Dotto, C. B. S., Kleidorfer, M., Deletic, A., Rauch, W., and McCarthy, D. T.: Impacts of measured data uncertainty on urban
687 stormwater models, *J. Hydrol.*, 508, 28-42, <https://doi.org/10.1016/j.jhydrol.2013.10.025>, 2014.

688 DWA-A118E: Hydraulic Dimensioning and Verification of Drain and Sewer Systems. Ger. Assoc. Water Wastewater Waste,
689 2006.

690 Fatone, F., Szelağ, B., Kiczko, A., Majerek, D., Majewska, M., Drewnowski, J., and Łagód, G.: Advanced sensitivity analysis
691 of the impact of the temporal distribution and intensity of rainfall on hydrograph parameters in urban catchments, *Hydrol.*
692 *Earth Syst. Sci.*, 25, 5493–5516, <https://doi.org/10.5194/hess-25-5493-2021>, 2021.

693 Fong, T. and Chui, M.: Modeling and interpreting hydrological responses of sustainable urban drainage systems with
694 explainable machine learning methods, *Hydrol. Earth Syst. Sci.*, 25, 5839 – 5858. <https://doi.org/10.5194/hess-2020-460>,
695 2020.

696 Fraga, I., Cea, L., Puertas, J., Suárez, J., Jiménez, V., Jácome, A.: Global sensitivity and GLUE-based uncertainty analysis of
697 a 2D-1D dual urban drainage model, *J Hydrol Eng.*, 21, 04016004, [https://doi.org/10.1061/\(ASCE\)HE.1943-5584.0001335](https://doi.org/10.1061/(ASCE)HE.1943-5584.0001335),
698 2016.

699 Fu, G., Butler, D., Khu, S-T., Sun, S.: Imprecise probabilistic evaluation of sewer flooding in urban drainage systems using
700 random set theory, *Water Resour Res.*, 47. <https://doi.org/10.1029/2009WR008944>, 2011.

701 Fu, G., Butler, D.: Copula-based frequency analysis of overflow and flooding in urban drainage systems, *J. Hydrol.*, 510, 49–
702 58, <https://doi.org/10.1016/j.jhydrol.2013.12.006>, 2014.

703 Guo, K., Guan, M., Yu, D.: Urban surface water flood modelling – a comprehensive review of current models and future
704 challenges. *Hydrol. Earth Syst. Sci.*, 25, 2843–2860. <https://doi.org/10.5194/hess-25-2843-2021>, 2021.

705 Harrell, F.E.: *Regression Modeling Strategies: With Applications to Linear Models, Logistic Regression, and Survival*
706 *Analysis*. Springer Series in Statistics, New York. ISBN: 9781475734621, 2001.

707 Hettiarachchi, S., Wasko, C., Sharma, A. : Increase in flood risk resulting from climate change in a developed urban watershed
708 – the role of storm temporal patterns. *Hydrol. Earth Syst. Sci.*, 22, 2041–2056. <https://doi.org/10.5194/hess-22-2041-2018>,
709 2018.

710 Hung, W., Hobbs, F. B.: How can learning-by-doing improve decisions in stormwater management? A Bayesian-based
711 optimization model for planning urban green infrastructure investments. *Environ Modell Softw*, 113, 59 – 72.
712 <https://doi.org/10.1016/j.envsoft.2018.12.005>, 2019.

713 Jato-Espino, D., Sillanpää, N., Andrés-Doménech, I., Rodríguez-Hernandez, J.: Flood Risk Assessment in Urban Catchments
714 Using Multiple Regression Analysis, *J. Water Resour. Plan. Manag.*, 144, 04017085, [https://doi.org/10.1061/\(asce\)wr.1943-](https://doi.org/10.1061/(asce)wr.1943-)
715 [5452.0000874](https://doi.org/10.1061/(asce)wr.1943-5452.0000874), 2018.

716 Jiang, Y., Zevenbergen, C., Mab, Y.: Urban pluvial flooding and stormwater management: A contemporary review of China’s
717 challenges and “sponge cities” strategy, *Environ Sci Policy*. 80, 132 – 143. <https://doi.org/10.1016/j.envsci.2017.11.016>, 2018.

718 Karamouz M, and Nazif S (2013). “Reliability-based flood management in urban watersheds considering climate change
719 impacts.” *J. Water Resour. Plann. Manage*, [http://doi.org/10.1061/\(ASCE\)WR.1943-5452.0000345](http://doi.org/10.1061/(ASCE)WR.1943-5452.0000345), 520–533.

720 Ke, Q., Bricker, J., Tian, Z., Guan, G., Cai, H., Huang, X., Yang, H., Liu, J.: Urban pluvial flooding prediction by machine
721 learning approaches – a case study of Shenzhen city, China, *Adv. Water Resour.*, 145, 103719,
722 <http://doi.org/10.1016/j.advwatres.2020.103719>, 2020.

723 Kelleher, C., McGlynn, B., and Wagener, T.: Characterizing and reducing equifinality by constraining a distributed catchment
724 model with regional signatures, local observations, and process understanding, *Hydrol. Earth Syst. Sci.*, 21, 3325– 3352,
725 <https://doi.org/10.5194/hess-21-3325-2017>, 2017.

726 Khan, M.P., Hubacek, K., Brubaker, K.L., Sun, L., Moglen, G.E. : Stormwater Management Adaptation Pathways under
727 Climate Change and Urbanization. *J. Sustainable Water Built Environ*, 8, 04022009.
728 <https://doi.org/10.1061/JSWBAY.0000992>, 2022.

729 Kiczko, A., Szeląg, B., Koziół, A.P., Krukowski, M., Kubrak, E., Kubrak, J., Romanowicz, R.J.: Optimal capacity of a
730 stormwater reservoir for flood peak reduction, *J. Hydrol. Eng.*, 23:04018008, [https://doi.org/10.1061/\(ASCE\)HE.1943-](https://doi.org/10.1061/(ASCE)HE.1943-)
731 [5584.0001636](https://doi.org/10.1061/(ASCE)HE.1943-5584.0001636), 2018.

732 Kim, Y., Eisenberg, D.A., Bondank, E.N., Chester, M.V., Mascaro, G., Underwood, S.: Fail-safe and safe-to-fail adaptation:
733 decision-making for urban flooding under climate change. *Clim Change*, 145, 397 – 412. <https://doi.org/10.1007/s10584-017->
734 [2090-1](https://doi.org/10.1007/s10584-017-2090-1), 2015.

735 Kirshen, P., Caputo, L., Vogel, R.M., Mathisen, P., Rosner, A., Renaud, T.: Adapting urban infrastructure to climate change:
736 a drainage case study, *J. Water Resour. Plan. Manag.*, 141, 04014064, [https://doi.org/10.1061/\(ASCE\)WR.1943-5452.0000443](https://doi.org/10.1061/(ASCE)WR.1943-5452.0000443),
737 2015.

738 Knighton, J., Lennon, E., Bastidas, L., White, E.: Stormwater detention system parameter sensitivity and uncertainty analysis
739 using SWMM, *J. Hydrol. Eng.*, 21, 05016014, [https://doi.org/10.1061/\(ASCE\)HE.1943-5584.0001382](https://doi.org/10.1061/(ASCE)HE.1943-5584.0001382), 2016.

740 Kobarfard, M., Fazloula, R., Zarghami M., Akbarpour: Evaluating the uncertainty of urban flood model using glue approach.
741 *Urban Water J*, 19, 600 – 615. <https://doi.org/10.1080/1573062X.2022.2053865>, 2022.

742 Lense, G.H.E., Lämmle, L., Ayer, J.E.B., Lama, G.F.C., Rubira, F.G., Mincato, R.L.: Modeling of Soil Loss by Water Erosion
743 and Its Impacts on the Cantareira System, Brazil. *Water*, 15, 1490. <https://doi.org/10.3390/w15081490>, 2023

744 Lama, G.F.C., Crimaldi, M., De Vivo, A., Chirico, G.B., Sarghini, F.: Eco-hydrodynamic characterization of vegetated flows
745 derived by UAV-based imagery, 2021 IEEE International Workshop on Metrology for Agriculture and Forestry
746 (MetroAgriFor), 273–278. <https://doi.org/10.1109/MetroAgriFor52389.2021.9628749>, 2021a.

747 Lama, G.F.C., Rillo Migliorini Giovannini, M., Errico, A., Mirzaei, S., Chirico, G.B., Preti, F.: The impacts of Nature Based
748 Solutions (NBS) on vegetated flows' dynamics in urban areas, 2021 IEEE International Workshop on Metrology for
749 Agriculture and Forestry (MetroAgriFor), 58–63. doi:10.1109/MetroAgriFor52389.2021.9628438), 2021b.

750 Lei, X., Chen, W., Panahi, M., Falah, F., Rahmati, O., Uuemaa, E., Kalantari, Z., Ferreira, C.S.S., Rezaie, F., Tiefenbacher,
751 J.P., Lee, S., Bian, H.: Urban flood modeling using deep-learning approaches in Seoul, South Korea. *J Hydrol*, 601, 126684.
752 <https://doi.org/10.1016/j.jhydrol.2021.126684>, 2021.

753 Li, X., Willems, P.: A Hybrid Model for Fast and Probabilistic Urban Pluvial Flood Prediction, *Water Resour. Res.*, 56,
754 e2019WR025128, <https://doi.org/10.1029/2019WR025128>, 2020.

755 Ma, B., Wu, Z., Hu, C., Wang, H., Xu, H., Yan, D., Soomro, S. : Process-oriented SWMM real-time correction and urban
756 flood dynamic simulation. *J Hydrol*, 605, 127269. <https://doi.org/10.1016/j.jhydrol.2021.127269>, 2022.

757 Martins, R., Leandro, J., Djordjević, S.: Influence of sewer network models on urban flood damage assessment based on
758 coupled 1D/2D models. *J. Flood Risk Manag.* 11, 717 – 728. <https://doi.org/10.1111/jfr3.1224>, 2018.

759 Mignot, E., Li, X., Dewals, B.: Experimental modelling of urban flooding: A review, *J. Hydrol.*, 568, 334-342.
760 <https://doi.org/10.1016/j.jhydrol.2018.11.001>, 2019.

761 Miller, J., Kim, H., Kjeldsen, T.R., Packman, J., Grebby, S., Dearden, R.: Assessing the impact of urbanization on storm runoff
762 in a peri-urban catchment using historical change in impervious cover. *J Hydrol*, 515, 59 – 70.
763 <https://doi.org/10.1016/j.jhydrol.2014.04.011>, 2014.

764 Mohammad, L., Bandyopadhyay, L., Sk, R., Mondal, I., Nguyen, T.T., Lama, G.F.C., Ahn, D.T.: Estimation of agricultural
765 burned affected area using NDVI and dNBR satellite-based empirical models. *J Environ Manage*, 343, 118226.
766 <https://doi.org/10.1016/j.jenvman.2023.118226>, 2023.

767 Morio, J.: Global and local sensitivity analysis methods for a physical system, *Eur. J. Phys.*, 32, 1577–1583,
768 <https://doi.org/10.1088/0143-0807/32/6/011>, 2011.

769 Ray, R., Das, A., Hasan, M.S.U., Aldrees, A., Islam, S., Khan, M.A., Lama, G.F.C.: Quantitative Analysis of Land Use and
770 Land Cover Dynamics using Geoinformatics Techniques: A Case Study on Kolkata Metropolitan Development Authority
771 (KMDA) in West Bengal, India. *Remote Sens*, 15, 959. <https://doi.org/10.3390/rs15040959>, 2023.

772 Razavi, S., Gupta, H.V.: A multi – method Generalized Global Sensitivity Matrix approach to accounting for the dynamical
773 nature of earth and environmental systems models, *Environ. Model. Softw.*, 114, 1 – 11.
774 <https://doi.org/10.1016/j.envsoft.2018.12.002>, 2019.

775 Romanowicz, R.J., Beven, K.J.: Comments on generalised likelihood uncertainty estimation, *Reliab. Eng. Syst. Saf.*, 91, 1315–
776 1321, <https://doi.org/10.1016/j.res.2005.11.030>, 2006.

777 Rosenzweig, B.R., Cantis, H., Kim, Y., Cohn, A., Grove, K., Brock, J., Yesuf, J., Mistry, P., Welty, C., McPhearson, T., Sauer,
778 J., Chang, H: The value of urban flood modeling. *Earth's Future*, 9, e2020EF001739. <https://doi.org/10.1029/2020EF001739>,
779 2021.

780 Shafizadeh-Moghadam, H., Valavi, R., Shahabi, H., Chapi, K., Shirzadi, A.: Novel forecasting approaches using combination
781 of machine learning and statistical models for flood susceptibility mapping. *J Environ Manage*, 217, 1 – 11.
782 <https://doi.org/10.1016/j.jenvman.2018.03.089>, 2018.

783 Shrestha, A., Mascaro, G., Garcia, M.: Effects of stormwater infrastructure data completeness and model resolution on urban
784 flood modeling. *J Hydrol*, 607, 127498. <https://doi.org/10.1016/j.jhydrol.2022.127498>, 2022.

785 Siekmann, M., Vomberg, N., Mirgartz, M., Pinnekamp, J., Mühle, S. : Multifunctional Land use in Urban Spaces to Adapt
786 Urban Infrastructure, 611 – 625. In: *Climate Change and the Sustainable Use of Water Resources*, 2011.

787 Siekmann, M., Pinnekamp, J.: Indicator based strategy to adapt urban drainage systems in regard to the consequences caused
788 by climate change, in: *12th International Conference on Urban Drainage*. pp. 11–16., 2011.

789 Sonavane N., Rangari, V.A., Waikar, M.L., Patil, M.: Urban storm-water modeling using EPA SWMM – a case study of Pune
790 city. *2020 IEEE Bangalore Humanitarian Technology Conference (B-HTC)*. 10.1109/B-HTC50970.2020.9297900, 2020.

791 Sun, Y., Liu, Ch., Du, X., Yang, F., Yao, Y., Soomro, S., Hu, C.: Urban storm flood simulation using improved SWMM based
792 on K-means clustering of parameter samples. *J Flood Risk Manag.* e12826. <https://doi.org/10.1111/jfr3.12826>, 2022.

793 Szeląg, B., Suligowski, R., Drewnowski, J., De Paola, F., Fernandez – Morales, F.J., Bąk, Ł.: Simulation of the number of
794 storm overflows considering changes in precipitation dynamics and the urbanisation of the catchment area: A probabilistic
795 approach, *J. Hydrol.*, 598, 126275, <https://doi.org/10.1016/j.jhydrol.2021.126275>, 2021b.

796 Szeląg, B., Kiczko, A., Łagód, G., De Paola, F.: Relationship between rainfall duration and sewer system performance
797 measures within the context of uncertainty, *Water Res Manage.*, 35, 5073 – 5087, [https://doi.org/10.1007/s11269-021-02998-](https://doi.org/10.1007/s11269-021-02998-x)
798 x, 2021.

799 Szeląg, B., Suligowski, R., De Paola, F., Siwicki, P., Majerek, D., Łagód, G.: Influence of urban catchment characteristics and
800 rainfall origins on the phenomenon of stormwater flooding: Case study, *Environ. Model. Softw.*, 150, 105335,
801 <https://doi.org/10.1016/j.envsoft.2022.105335>, 2022a.

802 Szeląg, B., Majerek, D., Kiczko, A., Łagód, G., Fatone, F., McGarity, A.: Analysis of sewer network performance in context

803 of modernization: modeling, sensitivity, uncertainty analysis. 12, 148. [http://doi.org/10.1061/\(ASCE\)WR.1943-](http://doi.org/10.1061/(ASCE)WR.1943-)
804 5452.0001610.

805 Taromideh, F., Fazloulou, R., Choubin, B., Emadi, A., Berndtsson, R.: Urban Flood-Risk Assessment: Integration of Decision-
806 Making and Machine Learning. *Sustainability*, 14, 4483. <https://doi.org/10.3390/su14084483>, 2022.

807 Thorndahl, S.: Stochastic long term modelling of a drainage system with estimation of return period uncertainty, *Water Sci*
808 *Technol.*, 59, 2331–2339, <https://doi.org/10.2166/wst.2009.305>, 2009.

809 Ursino, N.: Reliability analysis of sustainable storm water drainage systems. *WIT Transactions on The Built Environment*,
810 139, 149 – 157. <https://doi.org/10.2495/UW140131>, 2014.

811 Yang, Y., Chui, T.F.M.: Modeling and interpreting hydrological responses of sustainable urban drainage systems with
812 explainable machine learning methods, *Hydrol. Earth Syst. Sci.*, 25, 5839–5858, <https://doi.org/10.5194/hess-25-5839-2021>,
813 2020.

814 Yang, Q., Ma, Z., Zhang, S.: Urban Pluvial Flood Modeling by Coupling Raster-Based Two-Dimensional Hydrodynamic
815 Model and SWMM. *Water*, 14, 1760. <https://doi.org/10.3390/w14111760>, 2022.

816 Walek, G.: Wpływ dróg na kształtowanie spływu powierzchniowego w obszarze zurbanizowanym na przykładzie zlewni rzeki
817 Silnicy w Kielcach. Jan Kochanowski University Press, Kielce (in Polish), 2019.

818 Wu, J.Y., Thompson, J.R., Kolka, R.K., Franz, K.J., Stewart, T.W.: Using the Storm Water Management Model to predict
819 urban headwater stream hydrological response to climate and land cover change. *Hydrol. Earth Syst. Sci.*, 17, 4743–4758,
820 <https://doi.org/10.5194/hess-17-4743-2013>, 2013.

821 Venvik, G., Bang – Kittilsen, A., Boogaard, F. C.: Risk assessment for areas prone to flooding and subsidence: a case study
822 from Bergen, Western Norway. *Hydrology Research*, 51, 322 – 338. <https://doi.org/10.2166/nh.2019.030>, 2021.

823 Zhang, W., and Li, T.: The influence of objective function and acceptability threshold on uncertainty assessment of an urban
824 drainage hydraulic model with generalized likelihood uncertainty estimation methodology, *Water Resour. Manag.*, 29, 2059-
825 2072, <https://doi.org/10.1007/s11269-015-0928-8>, 2015.

826 Zhou, Y., Shen, D., Huang, N., Guo, Y., Zhang, T., Zhang, Y.: Urban flood risk assessment using storm characteristic
827 parameters sensitive to catchment-specific drainage system. *Sci. Total Environ.* 659, 1362–1369.
828 <https://doi.org/10.1016/j.scitotenv.2019.01.004>, 2019.

829

830